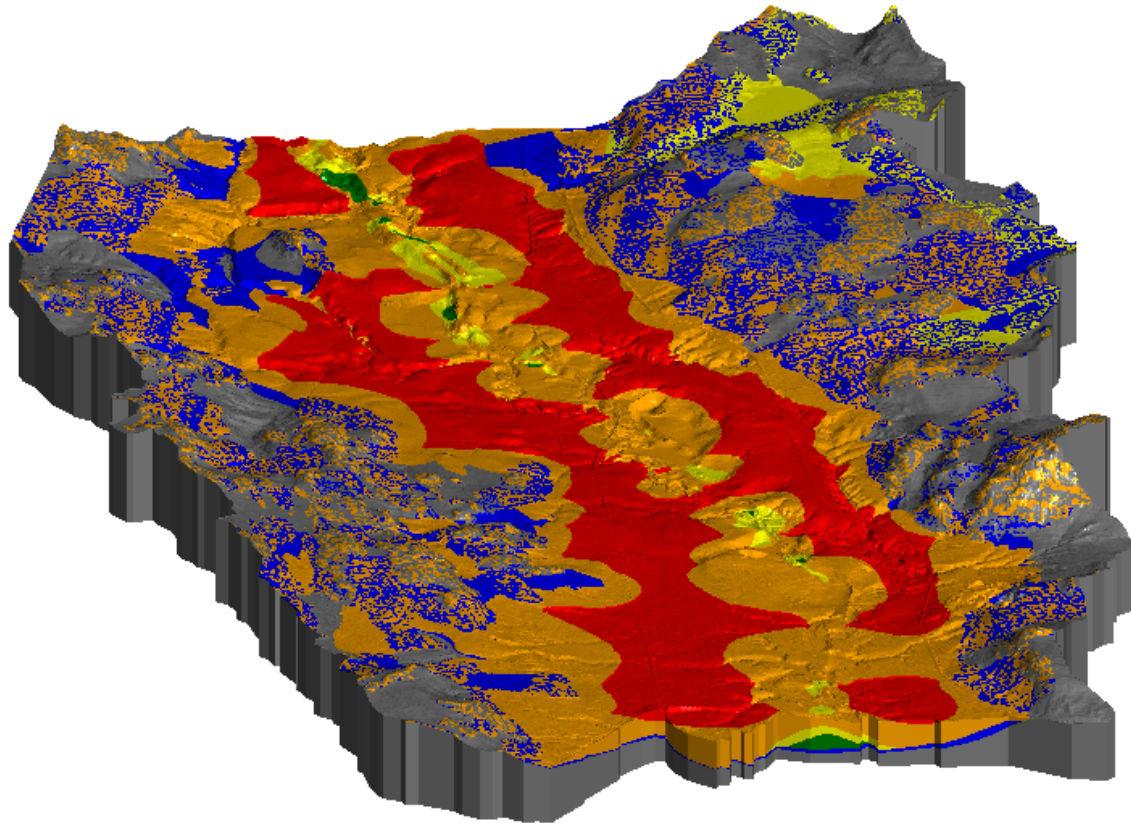




CHALMERS
UNIVERSITY OF TECHNOLOGY



Evaluating the Impact of Uncertainties in Groundwater Modelling

A case study of a glaciofluvial deposit investigating the effects of different boundary conditions using multiple numerical models

Master's thesis in Infrastructure and Environmental Engineering

KLARA DJERF

JOSEFIN HASSELBERG

DEPARTMENT OF ARCHITECTURE AND CIVIL ENGINEERING

CHALMERS UNIVERSITY OF TECHNOLOGY

Gothenburg, Sweden 2023

www.chalmers.se

MASTER'S THESIS 2023

Evaluating the Impact of Uncertainties in Groundwater Modelling

A case study of a glaciofluvial deposit investigating the effects of different
boundary conditions using multiple numerical models

KLARA DJERF

JOSEFIN HASSELBERG



CHALMERS
UNIVERSITY OF TECHNOLOGY

Department of Architecture and Civil Engineering
Division of Geology and Geotechnics
Engineering Geology
CHALMERS UNIVERSITY OF TECHNOLOGY
Gothenburg, Sweden 2023

Evaluating the Impact of Uncertainties in Groundwater Modelling
A case study of a glaciofluvial deposit investigating the effects of different boundary conditions using multiple numerical models
KLARA DJERF
JOSEFIN HASSELBERG

© KLARA DJERF, JOSEFIN HASSELBERG, 2023.

Supervisor: Johanna Merisalu, Department of Architecture and Civil Engineering
Examiner: Lars Rosen, Department of Architecture and Civil Engineering

Master's Thesis 2023
Department of Architecture and Civil Engineering Division of Geology and Geotechnics
Engineering Geology
Chalmers University of Technology
SE-412 96 Gothenburg
Telephone +46 31 772 1000

Cover: Visualisation of the geological groundwater model, presented in the program Leapfrog.

Typeset in L^AT_EX
Printed by Chalmers Reproservice
Gothenburg, Sweden 2023

Evaluating the Impact of Uncertainties in Groundwater Modelling

A case study of a glaciofluvial deposit investigating the effects of different boundary conditions using multiple numerical models

KLARA DJERF, JOSEFIN HASSELBERG

Department of Architecture and Civil Engineering Division of Geology and Geotechnics
Chalmers University of Technology

Abstract

The demand for drinking water is constantly increasing around the world, which partly entails an increased demand for groundwater of decent quality and quantity. Since groundwater is hidden beneath the ground, it is difficult to obtain a detailed comprehension of the hydrogeological conditions of an aquifer system. Groundwater modelling is a useful tool to increase the understanding of a current groundwater system and can be used to simulate future scenarios and events. The aim of this thesis is to set up several groundwater models and evaluate the impact of uncertainties regarding the conceptual understanding of boundary conditions. The models are based on an aquifer system located in a glaciofluvial deposit outside of Umeå Municipality (Sweden), where several geological and hydrogeological investigations have been conducted. Based on a conceptual model of the study area, a numerical model is set up with MODFLOW2005, to analyse how different boundary conditions affect the model results. Manual calibration is performed on parameter values and sensitivity analysis of different boundary conditions. The findings indicate that all the examined boundary conditions are viable for utilization; nevertheless, it should be noted that there can be considerable variations in the obtained results. Uncertainties in the conceptual model, and the numerical model, are discussed and ideas for further studies are presented. In conclusion, the geological model is the key conceptual uncertainty. All boundary condition combinations that were tested are applicable, with the most significant differences emerging during pumping events when the system is stressed. An understanding of the system and the model itself is essential for identifying uncertainties and recognising their impact on the modelling results.

Keywords: Groundwater modelling, Groundwater model uncertainty, Conceptual model, Numerical model, MODFLOW2005, Flopy, Glaciofluvial deposit

Acknowledgements

This thesis is the final part of the Master Program Infrastructure and Environmental Engineering at the department of Architecture and Civil Engineering, Chalmers University and was conducted during the spring of 2023. The thesis has been conducted in cooperation with Water Resources at Ramboll Sverige. We would like to thank all the people in the water resources group in Gothenburg at Ramboll, especially Oskar Sjöberg for helping us with GIS and for creating the Leapfrog model, Christian Nielsen for help with conceptualisation, and Per Sander for supporting us with knowledge about the area, geology, and great comments on the report. We would also like to thank our examiner Lars Rosén and the research group Engineering Geology at ACE. We would also like to give a special thanks to our supervisor Johanna Merisalu for your guidance and support. Lastly, a special thanks to Nils Hammaräng Grip for Python-support.

Klara Djerf and Josefin Hasselberg, Gothenburg, June 2023

Contents

List of Figures	xi
List of Tables	xiii
1 Introduction	1
1.1 Aim	2
1.2 Limitations	2
1.3 Thesis structure	3
2 Theory, Methods, and Concepts	4
2.1 Groundwater Modelling	4
2.2 Conceptual Models	5
2.3 Numerical Groundwater Models	7
2.4 Boundary Conditions	8
2.5 MODFLOW	9
2.6 Calibration	10
2.7 Uncertainties	10
2.7.1 Uncertainty Sources	11
2.7.2 Uncertainty Analysis	12
2.7.3 Sensitivity Analysis	12
3 Case Study Application	14
3.1 General Description of Case Study Area	14
3.2 Geology	16
3.3 Geological Model Development	19
3.4 Model Area	22
3.5 Hydrogeology and Groundwater Recharge	22
3.6 Boundary Conditions	26
3.6.1 Boundary Conditions along the Edges of the Model Area	27
3.6.2 Boundary Conditions within the Model Area	28
3.7 Multiple Groundwater Models	29
4 Numerical Model Development	31
4.1 Discretisation	31
4.2 Geology	32
4.3 Hydrogeology and Groundwater Recharge	32
4.4 Boundary Conditions	33
4.5 Pumping	34
4.6 Model Run	35

4.7	Calibration	35
4.8	Multiple Groundwater Models	36
4.9	Result Analysis	36
5	Results	37
5.1	Pumping	41
6	Discussion	44
6.1	Calibration	44
6.2	Conceptual errors	45
6.3	Sensitivity Analysis of the Impact of Boundary Conditions	46
6.3.1	The Impact of Pumping Event	47
6.3.2	Summary of the Impact of Boundary Conditions	48
6.4	Uncertainties in Groundwater Modelling	48
6.5	Further Studies	48
7	Conclusion	50
	References	53
A	Appendix A - Calibration Results	I
B	Appendix B - Flopy Script	III

List of Figures

2.1	Groundwater modelling process, with inspiration from Anderson, Woessner, and Hunt (2015).	5
3.1	Overview map of case study area, located in Vännäs in the north of Sweden.	14
3.2	Overview map of the subcatchment area of <i>Umeälven</i> and the subcatchment area of <i>Tvärån</i>	15
3.3	General illustration of groundwater in a glaciofluvial deposit, similar to Umeälvsåsen (Wikner, Müllern, Rurling, & Thunholm, 2002a).	17
3.4	Soil type map from SGU over Umeälvsåsen and the subcatchment area. . .	18
3.5	One cross-section profile of the esker, created based on knowledge about deposition environment, boreholes and seismic investigations. To the left, a zoomed in figure of how the borehole data and seismic result has been transferred to 5 different soil layers in the profile. The outer part of the profile is only based on knowledge about the geology in the area	19
3.6	Geological model created in Leapfrog. Some of the profiles, which the model is created by, is shown as white lines crossing the model.	20
3.7	A cross-section of the geological model in Leapfrog from the south part of the area. Including a legend over the different soil types. The esker is clearly visible in the middle of the cross-section as the green/yellow ridge. .	21
3.8	A cross-section of the geological model in Leapfrog from the north-middle part of the area. Including a legend over the different soil types. Showing a very thin layers of sand and gravel and a thick layer of semi-fines.	21
3.9	A cross-section of the geological model in Leapfrog from the north boundary of the area. Including a legend over the different soil types. Showing a very thick layer of till below the sand and gravel.	21
3.10	Overview map of the model area with the soil type map visual in the background. The model area is based on the catchment area.	22
3.11	Map over catchment area with illustrations of the groundwater flow directions. Including a legend describing the different arrows and colours in the map.	24
3.12	Observation wells located in the model area. All observation wells are located along the esker. The orange polygons illustrating the division of observation wells in three zones.	25
3.13	Histogram of hydraulic conductivity values of gravel and sand.	26
3.14	Normal distribution of hydraulic conductivity of gravel and sand.	26
3.15	Locations of boundary conditions within the model area. Including a legend presenting different boundary conditions and the model area. The boundary conditions are located at the edges of the model area, in three sections named A, B, and C.	28

3.16	The location of Boundary condition D illustrating the river Tvärån in the model area. The Boundary condition D going through the whole model area from north-south.	29
4.1	A Cross-section of the Leapfrog model with the grid and soil layers visible. To the right a zoomed-in column from the grid illustrating that the same soil type is assigned to several layers in the model.	32
4.2	Conceptualisation of numerical model and location of different boundary conditions A,B, C, and D. Illustrated in QGIS. The legend is showing the colours for different boundary conditions, active and inactive cells, and the pumping wells.	34
5.1	Simulated head from all 12 models plotted together with observed head in several observation wells from north to south in the model area. Observed values are marked with a black line and the models with the same boundary conditions are colour matched. All models with drain has solid lines and those without drain has dashed lines.	38
5.2	Cross-sections (west-east) of model SFS-D at three different locations in the model.	39
5.3	Cross-sections (west-east) of model FFS-ND at three different locations in the model.	40
5.4	Drawdown for all models after pumping in three pumping wells; B1N, BM4 and B2S. Models with drain is marked with solid lines and models without with dashed lines. Models with the same boundary conditions are color matched.	41
5.5	Drawdown for models with drain included after pumping in three pumping wells; B1N, BM4, B2S.	42
5.6	Contour plot of drawdown for Model FSS-D. Contours mark the drawdown as lines and a blue color indicates the areas with largest drawdown.	43
5.7	Contour plot for drawdown for Model FFS-D. Contours mark the drawdown as lines and a blue color indicates the areas with largest drawdown.	43

List of Tables

2.1	Framework for conceptual modelling. Inspired by Brassington and Younger (2010).	6
3.1	Principle stratigraphy of deposits below the highest coastline.	16
3.2	Hydraulic conductivity minimum, maximum, and mean, for all soil types.	26
3.3	Boundary conditions.	26
3.4	All groundwater models with different boundary conditions and their names.	30
A.1	Final hydraulic conductivity for each soil type.	I
A.2	Share of recharge for each soil type. 100 % is 350 mm / year.	I
A.3	Assigned inflow and outflow in the models with flow boundary.	I
A.4	Conductance for drainage.	II
A.5	Pumping rate in the three pumping wells in North, Middle and South. Presented in both l/s and m^3/d	II

1

Introduction

Water is the most important necessity for life on Earth. Clean water is not only vital for drinking and sanitation, but also essential in agriculture and other industries (Barthel et al., 2021). It is, therefore, a part of the Sustainable Development Goals, made by United Nations (2022). Goal number six, called *Clean water and sanitation*, is to ensure access to clean water for everyone, which includes prevention of water scarcity and improvement of drinking water management.

The access to fresh water for drinking water supply varies around the world, since it depends on local climate and geology conditions. The fresh water is either surface water or groundwater and stands for about 2.5 % of the total amount of water on Earth (U.S. Geological Survey, 2018). The demand for drinking water is constantly increasing due to the growth of population, agriculture, and industry (especially the energy sector) (U.S. Geological Survey, 2018). In Sweden, the accessibility of fresh water is generally good, and both surface water and groundwater is used to supply the population with drinking water. Today, 50 % of Swedish municipal water supplies are based on groundwater, half of which comes from natural groundwater and the other half from artificial groundwater (Svenskt Vatten, 2016). In large cities, it is common to use surface water as a fresh water source, since the withdrawal capacity from surface water is often greater than from aquifers. However, surface water can easily get contaminated by stormwater, agriculture runoff, construction, and industries etc. and is, therefore, of varying quality (D. Walker et al., 2019). Furthermore, the risk of contamination might increase in the future as a result of the growing population, urbanization and climate change. These activities cause releases of nutrients, pathogens, and plastics, among others that contaminates the water (Borthakur & Singh, 2020).

Since groundwater partly consists of infiltrated surface water, and since the ground itself can be contaminated, groundwater can also be of poor quality and may not be suitable as drinking water. However, the energy demand and use of chemicals are higher at a surface water treatment plant compared to the treatment of groundwater, since surface water has to be purified to a larger extent (Svenskt Vatten, 2019). This is due to the natural filtration that occurs in the soil when a groundwater system is recharged.

Managed Aquifer Recharge (MAR) is one way to take advantage of both surface water quantity and groundwater quality. By using artificial recharge, the amount of available groundwater in an aquifer can be increased (Fetter, 2014). To implement a MAR system, the hydraulic properties of the aquifer is of great importance. However, the knowledge of an aquifer is always limited due to natural variations, such as recharge and geological heterogeneity and the fact that the aquifer and groundwater are below the surface and thus to a large extent out of sight. Due to the natural variation and our limited knowledge

about it, assumptions needs to be made when conceptualising the project area, which leads to uncertainties and a limited understanding of the groundwater system.

Groundwater modelling is a useful tool to increase the understanding of groundwater flow within an aquifer and the system as a whole (Bakker & Post, 2022). Modelling can give us an understanding of the current situation by simplifying the complex reality and by using different equations to calculate different parameters from a range of measured input data. In a time of constant change, considering extensive infrastructure developments, climate change, and a growing population, it is also necessary to understand more about the future and to be able to make predictions. Mathematical models can use past and present data to calculate future scenarios that can help us understand the consequences of today's actions. Furthermore, models can help us understand hidden systems where limited amount of data exists, such as a complex aquifer system. However, due to the many sources of uncertainties in modelling, it is necessary to analyse how different uncertainties affect the mathematical model.

Umeå municipality in northern Sweden is growing and the demand for drinking water is expected to increase by 50 % in a near future. The municipality wants to implement an artificial groundwater recharge facility to expand their drinking water supply. In this thesis, a conceptual and a mathematical groundwater model is developed of an aquifer system in a glaciofluvial deposit outside of Umeå municipality, in Vännäs.

1.1 Aim

The overall aim of this study is to set up several groundwater models and evaluate the impact of uncertainties on the overall result. This will be done by performing a local sensitivity analysis of multiple models that are based on different conceptualisations regarding boundary conditions of the model area. Uncertainties in the models will be documented and analysed, with a local sensitivity analysis. This entails that one attribute will be changed at a time, to observe what impact that attribute has on the results. To meet the aim, the following research questions will be answered:

- What are the key conceptual uncertainties in defining conditions for the study area, and how do they affect the overall result?
- How do different boundary conditions in numerical groundwater models influence the resulting groundwater levels?
- How do numerical modelling uncertainties contribute to the overall uncertainty of groundwater model results?

1.2 Limitations

This thesis is focusing on the research questions and has the following limitations:

- The data that will be used in the thesis are based on previous investigations. No further investigation will be conducted during the thesis process.
- Water quality is not considered in this thesis.

1.3 Thesis structure

The following section provides an overview of the structure of this thesis, highlighting the key sections that constitute its framework. This structure has been designed to ensure a logical flow that matches the process of the thesis.

The thesis is divided into several main chapters, each serving a specific purpose in contributing to the overall understanding of the research subject. These chapters include:

- **Introduction:** This chapter presents the study area and highlights the significance of the research. It also outlines the aim, objectives, and limitations of the study.
- **Theory, Methods, and Concepts:** This chapter consists of a literature review on existing theories related to the research topic, as well as the methods and concepts employed for conducting the conceptual and numerical models and for assessing the results.
- **Case Study Application:** This chapter provides a general description of the case study area and presents the conceptual model. The conceptual model is presented in several parts, following the order of its creation.
- **Numerical Model Development:** This chapter details the development of the numerical model based on the conceptual model, following a structure similar to that of the conceptual model. The chapter also includes parameter calibration.
- **Results:** The results chapter describes the model results, presented in both text and figures.
- **Discussion:** The discussion section involves analyzing the results, addressing uncertainties, and examining the impact of different boundary conditions. It concludes with a general discussion on uncertainties in groundwater modeling.
- **Conclusion:** This chapter summarizes the main findings of the study and provides answers to the research questions.

2

Theory, Methods, and Concepts

The following chapter includes theory about the different steps of groundwater modelling, such as conceptual models, numerical models, calibration and uncertainties in the model. Used methods are also presented as well as important concepts for the work.

2.1 Groundwater Modelling

A model is a simplified version of a complex real system (Anderson et al., 2015). In hydrogeology, modelling is often used as a method to summarise known facts of the system in form of written text, figures, and tables, and to get a further understanding of aquifer conditions. Groundwater models are a crucial part of hydrogeology since aquifer response cannot be fully tested in the field (Bakker & Post, 2022). There are several types of groundwater models that fills different functions. Conceptual models are static models that describe what is known about a specific aquifer site. There are also several types of dynamic models that can investigate and describe movements in the aquifer, such as flow and flux. These can be divided into physical models and mathematical models (Fetter, 2014; Anderson et al., 2015). Physical models are mostly made in a laboratory scale, where tanks and columns can be filled with porous materials to test the hydraulic conductivity and flow of the system. Analog models are also physical models where electric current is used instead of water to study the flow in a system. However, both the physical scale models and the analog models have significant disadvantages (Fetter, 2014). It can require professional knowledge in carpentry, plumbing, and wiring, as well as a lot of space and funds to construct the models. Furthermore, the models are not extensively flexible and it can be difficult to change the characteristics. In mathematical models, on the other hand, parameters could easily be modified and are based on equations of flow, heat, and mass transport. These models can be data-driven or process-based (Anderson et al., 2015). Data-driven models use equations to calculate unknown variables from known data, while process-based models use governing equations, such as boundary conditions, which describes the physical process of a system. The mathematical models can then be solved analytically or numerically, depending on the complexity of the system. According to Zheng and Bennett (1995), it is necessary to use a numerical model when a groundwater system has complex boundary conditions or when there are varying parameter values within the model boundary.

Groundwater modelling is an iterative process where some steps might be redefined during the development of the final model (Anderson et al., 2015; Refsgaard et al., 2007; Butts et al., 2004). Figure 2.1 presents the steps in a groundwater modelling process. The first step is to define the purpose of the model and to decide which parameters and processes needs to be considered. Furthermore, the definition of the purpose can lead to

the formulation of specific research questions, which will generate a need for reasonable limitations in order to make a simple model. Simple models are generally quicker to solve computationally. Furthermore, they are easier to interpret and understand, thus easier to conduct an uncertainty analysis on. However, the level of complexity should be adjusted for the problem being addressed (El-Ghonemy et al., 2005). The next step is to create the conceptual model, which is further described in Section 2.2 Conceptual models. Based on the purpose of the model and the conceptual model, the mathematical model and code are decided (Section 2.3 Numerical Groundwater models). The model design step includes translating the conceptual model into the mathematical model. In this step, the model grid is designed, boundaries are defined, and parameter values are assigned. Furthermore, the calibration of the model can be an important part of developing a model, according to Anderson et al. (2015), and is described in section 2.6 Calibration. If the calibration is rejected, it is necessary to adjust the model design or improve the conceptual model to achieve an approved calibration. When the calibration is accepted, a base model is established and forecast simulations can be performed. The forecast simulations are used to simulate future events or responses of the system. In addition, uncertainties for the forecast simulations and the model has to be evaluated. Types and sources of uncertainties are further described in section 2.7 Uncertainties. Next step is to analyse the result gained from the simulations. However, if new data is available, the conceptual model should be updated and the following steps are then performed again. When the results are analysed, the report could be completed.

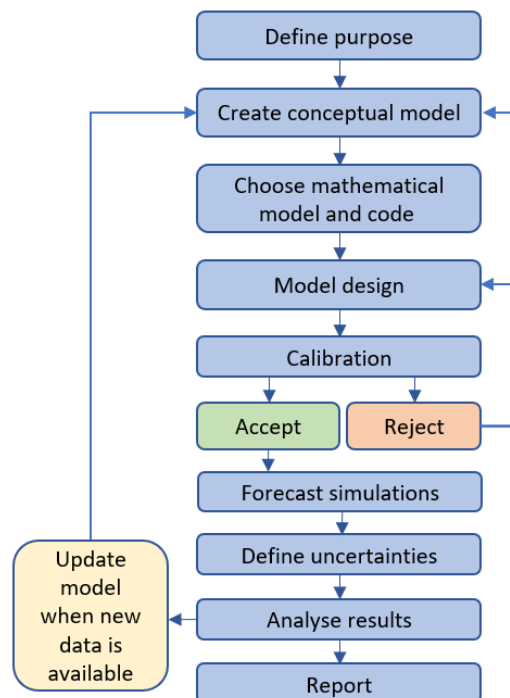


Figure 2.1: Groundwater modelling process, with inspiration from Anderson et al. (2015).

2.2 Conceptual Models

A conceptual model is a simplified description and presentation of a complex system (Enemark et al., 2019; Gupta et al., 2012; El-Ghonemy et al., 2005). Hydrogeological sys-

tems are complex due to spatial variation of properties, leading to different flow processes within an area. Therefore, the set-up of a conceptual model is essential for the groundwater modelling process to get a systematic overview and understanding of the site, in terms of structure and processes (Fetter, 2014). Additionally, it is not possible to examine the system in its entirety due to time and financial constraints. The conceptual model will therefore include several limitations and uncertainties.

The conceptual model development involves both the physical and process structures of the system, where the first includes behaviour of the system in absence of water and energy, whereas the process structure includes the processes that are mediated through the physical structure (Gupta et al., 2012). The development of a conceptual model is based on available data and knowledge about the hydrogeological characteristics of the system. According to Gupta et al. (2012), the degree of understanding depends on training and experience. The model is updated when more data and knowledge about the system is gained, which makes the development of a conceptual model an iterative process (Brassington & Younger, 2010). The conceptual model should be customised to the specific site and aim of the project. However, it is important to avoid making the model oversimplified or undersimplified (El-Ghonemy et al., 2005). A risk with an oversimplified model is that the model poorly represent reality and is missing important details. On the other hand, an undersimplified model is too complex to be able to build a numerical model. A framework for conceptual modelling is presented in Table 2.1.

Table 2.1: Framework for conceptual modelling. Inspired by Brassington and Younger (2010).

Steps	Activity	Description
1	Define objectives	Define aim, elements of study and research objectives.
2	Topography and hydrology	Identify water features, estimate catchment boundary. Conduct a topography analysis.
3	Geology	Collect and interpret geological, borehole, and geophysical data.
4	Aquifer framework	Interpret data from pumping tests. Define aquifer boundaries, spatial distribution and hydraulic properties.
5	Groundwater flow	Defining groundwater flow directions and hydraulic head.
6	Aquifer relationships	Assess relationship between groundwater levels, other aquifers and surface water bodies and quantify groundwater flow.
7	Water balance	Assess available groundwater resources using water balance.
8	Description of model	Perform a written description of the conceptual model with illustrations.

The process of developing a conceptual model contains several steps. Different guides and recommendations about building a conceptual model, and which data is required, is found in the literature. American Society for Testing and Materials (ASTM International) have a standard guide for conceptualisation of groundwater systems, including a step-wise proceeding framework and a checklist of required data (ASTM International, 2019). A similar framework is proposed by Brassington and Younger (2010), based on a compilation of available guidelines in selected hydrogeology publications. The steps should be performed in the right order since defined parameters and data from the step before is used in the next step. All of the steps contributes to the conceptual model and could be updated during the process of groundwater modelling when gaining more available data or knowledge. Table 2.1 above is based on the framework from Brassington and Younger (2010).

Similar to the whole groundwater modelling process, the first step in the framework is to define the aim and the research objectives of the conceptual model. Since a groundwater model is based on geological and hydrological information, the next step is to identify, collect, and define available data from the site. Most of the data comes from field measurements from boreholes or geophysical investigations of different sections of the system. Collecting data from several points, in combination with interpretation of the data, leads to a preliminary understanding of the system. There is, however, a limited amount of data available from boreholes, thus a set of assumptions need to be made in order to build a model for further analysis (Zhou & Herath, 2017). If the assumptions are made with insufficient knowledge, it will lead to major uncertainties. According to several studies, the largest uncertainty in groundwater models comes from the conceptualisation (Bredehoeft, 2005; Rojas et al., 2010; Zhou & Herath, 2017).

2.3 Numerical Groundwater Models

As earlier mentioned, mathematical models can be solved numerically when a process-based groundwater model has complex boundary conditions or when parameter values differ within the boundaries (Fetter, 2014; Anderson et al., 2015). Process-based models that are based on groundwater flow are built from the principles of mass conservation and Darcy's law, which states that water is neither created or destroyed and that water flows from high to low potential energy. These principles are the basis of the governing equations of the mathematical model, which are listed below in Equation 2.1, 2.2, 2.3, and 2.4, which are all taken from Anderson et al. (2015).

Darcy's law:

$$\frac{q}{A} = -\frac{k}{\mu} \frac{\delta P}{L} \quad (2.1)$$

where: q Flow.
A Area.
k Permeability.
 μ Fluid viscosity.
 δP Pressure drop.
L Length of medium.

Water balance equation:

$$\frac{\delta q_x}{\delta x} + \frac{\delta q_y}{\delta y} + \frac{\delta q_z}{\delta z} - W^* = -S_s \frac{\delta h}{\delta t} \quad (2.2)$$

where: q_x, q_y, q_z Flux/flow rate in different axes.
 W^* Volumetric inflow rate from sources and sinks.
 S_s Specific storage (volume of water released from storage per unit change in head, h).
 t Time.

To simplify Equation 2.2 for practical use, the components of the specific discharge vector, q , can be rewritten as:

$$\begin{aligned} q_x &= -K_x \frac{\delta h}{\delta x} \\ q_y &= -K_y \frac{\delta h}{\delta y} \\ q_z &= -K_z \frac{\delta h}{\delta z} \end{aligned} \quad (2.3)$$

When equation 2.3 is substituted into 2.2, it gives the general governing equation (differential equation) that represents 3D transient groundwater flow for heterogeneous and an-isotropic conditions:

$$\frac{\delta}{\delta x} (K_x \frac{\delta h}{\delta x}) + \frac{\delta}{\delta y} (K_y \frac{\delta h}{\delta y}) + \frac{\delta}{\delta z} (K_z \frac{\delta h}{\delta z}) = S_s \frac{\delta h}{\delta t} - W^* \quad (2.4)$$

where: K The hydraulic conductivity tensor.

As earlier mentioned, the boundary conditions can be quite complex in a numerical model in consequence of the governing equations. These can then be solved with numerical methods, such as the finite elementary (FE) or the finite differential (FD) method (Anderson et al., 2015). The FE method divides the domain (model area) into small elements where the solution is approximated over each element and seeks to minimize the error by solving a system of equations. Whereas the FD method divides the domain into a grid of points where the solution is approximated by finite differences between the points and seeks to solve a system of equations that relates values of unknown functions for each point. The FE method is appropriate to use for more complex boundary conditions, however, the FD method is simpler to implement and does not need as much computational capacity.

2.4 Boundary Conditions

The model also consists of boundary conditions, which can be explained as processes along the boundaries or along sources and sinks inside of the model domain (Anderson et al., 2015). These can be divided into three types, which will have different effects on the hydrogeology in the model:

- Dirichlet conditions - Specified head boundary, where the head (groundwater level) is set to a specific value along the boundary.

- Neumann conditions - Specified flow boundary, where the derivative of the head is set along the boundary.
- Cauchy conditions - Head-dependent boundary, where the boundary crossing flow is calculated from the gradient between a set head outside of the model domain and the computed head within the domain.

If a head boundary is used, the boundary crossing flow will be calculated or set. Whereas, if a flow boundary is used, the head will be calculated when running the model. The important difference between a specified head boundary and a head-dependant boundary is that the first mentioned head is maintained throughout the simulation period (USGS, n.d.). However, a head-dependent head boundary will have a varying head over time.

Furthermore, there are conditions in some model boundaries where a no-flow boundary can be assumed. This can happen when the boundary has a perpendicular direction against the groundwater level contours in an area, i.e. a water divide. No-flow can also be assumed when some type of groundwater divider occurs.

2.5 MODFLOW

The boundary conditions, together with the governing equations, can be inserted into a number of different GUI's (Graphical User Interfaces), such as the modelling software's, Groundwater Modeling System (GMS), Visual Modflow and Groundwater Vistas (Bakker et al., 2016). The GUI formats and assembles data, creates input files, executes code, and can also process output files (Anderson et al., 2015). The most commonly used underlying FD code in GUI's is called MODFLOW, which is a numerical modelling software (Leaf & Fienen, 2022). It can also be described as a groundwater flow model whose input values are not yet defined. An alternative method to using a GUI is to use a programming language, such as Python, to make a MODFLOW model (Bakker et al., 2016). The same underlying code and governing equations are used with another interface.

Python has a package, called FloPy, which is a set of tools that allows the user to import and define parameters, the FD grid, and boundary conditions in a domain to build a numerical model (Bakker et al., 2016). The script writes the input files for MODFLOW and can then be used to run the model and present results as binary model output and customised plots. To be able to create a script, there are a number of steps that could be followed. The following steps are inspired from Bakker et al. (2016).

1. Import FloPy and other packages
2. Create a MODFLOW model
3. Define the model set up, including discretisation and boundary conditions
4. Define the model stress period data
5. Define the model solver and solution method to obtain heads
6. Generate the MODFLOW input files to disk
7. Run the model
8. Calibration

2.6 Calibration

To be able to validate that a numerical model does not contain false assumptions and that the chosen boundary conditions match reality, it is necessary to calibrate the model (Tonkin & Doherty, 2009). This is done by comparing the model results to available data from the site. Parameters, such as hydraulic conductivity and recharge rate, can then be adjusted to match the measured values. It is possible to calibrate the model towards groundwater levels in a steady state or towards measured values from a pumping test, as long as the outflow from the pumping test is included to get the water budget as close to zero as possible in the model (Anderson et al., 2015).

If the model contains accurate processes, potential errors in predictions could depend on parameter values. Since it can be difficult to assume the correct parameter values, the values could be calibrated by manual calibration or parameter estimation computationally. A common software used for parameter estimation is PEST (Model-Independent Parameter Estimation and Uncertainty Analysis) (Doherty, 2003). The method gives optimal parameter values and calibration statistics. Another method for calibration is manual calibration, which is widely used to calibrate models (Boyle et al., 2000). This is when measured values are manually compared to the results from the model. The model parameters are thereafter changed until the simulated results correspond to the measured values. Manual calibration is labor intensive, however, one advantage is to have control over the parameters and to understand which parameters affect the model results.

2.7 Uncertainties

In groundwater models and modelling, uncertainty is one major factor to consider when evaluating the result and the quality of the model. Uncertainties comes from several different sources and arises for various reasons. Input and output data from the model can be unreliable, due to sampling errors, misinterpretation of the data, lack of knowledge about how to use the data, and many other reasons. As earlier mentioned, a complex natural system contains inherent variability, which can be a major cause of uncertainty in a model (W. Walker et al., 2003; Samani et al., 2018). However, the uncertainty is not just the absence of knowledge, unknown unknowns is a major part of uncertainty in models (Anderson et al., 2015). There are several methods to decrease the uncertainties in models and modelling. However, the uncertainty can never be completely eliminated (Anderson et al., 2015). Thus, awareness of how the uncertainty can influence the system is essential and it needs to be evaluated when the results are analysed. Moreover, it is important to document assumptions made in e.g the conceptual model for the evaluation of the results (El-Ghonemy et al., 2005).

In the literature, there are several ways to consider uncertainty and determine which sources are contributing to the uncertainty (Refsgaard et al., 2007). Uncertainty could be described in three dimensions, (i) Nature, (ii) Type, and (iii) Source (W. Walker et al., 2003; Refsgaard et al., 2007). According to W. Walker et al. (2003) and Refsgaard et al. (2007), the nature of uncertainty is divided into two parts; epistemic uncertainty and stochastic/aleatory uncertainty. Epistemic uncertainty is due to inadequate knowledge, which can be reduced by increasing the knowledge. Aleatory and stochastic uncertainties are due to inherent variability and unpredictability in the system (Gong et al., 2013).

The levels (or types) of uncertainty refers to a point on the spectrum between having clear,

deterministic knowledge and complete ignorance at which uncertainty becomes apparent (W. Walker et al., 2003). Historically, aleatory uncertainty has been the main uncertainty considered in natural science and modelling processes. A common uncertainty comes from measurement uncertainty due to sampling error. Moreover, scenario uncertainty is also a level of uncertainty to consider, since the future of the studied system entails a range of possible outcomes (Samani et al., 2018; Rojas et al., 2010). Furthermore, recognised ignorance is another type of uncertainty which implies that the ignorance of knowledge is partly reducible. The last type to consider is the total ignorance, which is irreducible since it is about the unknown unknowns.

2.7.1 Uncertainty Sources

The sources or locations of uncertainty refer to different parts of the modelling process where the uncertainty arises from. In modelling, there are several sources of uncertainty. The main ones are input data, parameters, model structure and model technical uncertainty (Refsgaard et al., 2007).

Input data

Uncertainty due to input data arises from the lack of data or data of poor quality that is not representative for the site (Refsgaard et al., 2007). It is therefore important to research what type and amount of data that is available and which data is necessary and relevant to include in the model. The more parameters that are included, the more complex the model becomes. Over-parameterization, meaning more parameters are included in the model than the data can represent, is problematic (Beisbart & Saam, 2019). It increases the uncertainty since the data is distributed through all parameters and if the data quality is lacking, it affects the model result (Engelhardt et al., 2014). However, too few parameters can make the model oversimplified and the risk is that the model will not be able to represent the actual processes in the system.

Parameter uncertainty

The parameter uncertainty is about parameter values and could include both aleatory and epistemic components (Refsgaard et al., 2007). Aleatory uncertainty arises from natural variability that is challenging to capture within parameter value data. The impact of variability in parameter values cannot be precisely determined or controlled. The epistemic component of parameter uncertainty refers to the uncertainty arising from a lack of knowledge due to limitations in available data or measurement errors. Data sampling errors can occur due to too few samples or non-representative samples.

Model structure, including the conceptual model

Thirdly, model structure uncertainty is one of the main uncertainties to consider in the groundwater modelling process. When conceptualising, a general understanding of the site is essential, since it is the base of all the assumptions that will be made in the model. An incomplete understanding of the geology and system inevitably contributes to the model structure uncertainty (W. Walker et al., 2003). The model structure also includes the boundaries, i.e. the extent of the system modelled and the relationship between input data and parameters. The boundary conditions and classification of aquifers are uncertain and is often simplified in a groundwater model. Furthermore, equations used to set up the model and the interactions between variables are considered within the model structure (W. Walker et al., 2003).

Model technical uncertainty

The model technical uncertainty refers to numerical approximations and errors in the software that is used (Refsgaard et al., 2007; W. Walker et al., 2003). Errors and bugs are difficult to reduce since they are integrated into the software code.

2.7.2 Uncertainty Analysis

To assess the uncertainties in a model, an uncertainty analysis should be performed. Uncertainty analysis is often performed at the end of the modelling process and is included in the groundwater modelling process (Figure 2.1) as the last step before the analysis of the result. However, according to Refsgaard et al. (2007), the uncertainties should be taken into account during the entire process to be able to minimize them and the modeler should be aware of the different uncertainties existing in the model. Refsgaard et al. (2007) have listed 13 different uncertainty analysis methods, and a few of them that could be connected to this project is presented below.

Monte Carlo simulations: is used to evaluate statistical uncertainty. By running a large number of simulations with random input parameters, Monte Carlo simulations can provide a range of possible outcomes and their probabilities, which can be used to quantify and characterize the uncertainty associated with a model.

Multi model simulation: refers to model structure uncertainty. By setting up several models with different structures, the model structure uncertainty could be analysed. This is normally performed by setting up different conceptual models based on geological assumptions.

Scenario analysis: is a tool to deal with scenario uncertainty. The analysis contains different possible futures and is made by simulating different scenarios. The goal of a scenario analysis is to identify the range of possible outcomes under different assumptions or conditions and to assess the risks and opportunities associated with each scenario.

Uncertainty matrix: is used to identify the most important uncertainties (W. Walker et al., 2003; Refsgaard et al., 2007). The matrix structures the uncertainties by source and type and each uncertainty gives a weighting based on how large the uncertainty is and how important the source is for the project context.

Expert elicitation: is a common supporting method for uncertainty analysis (Refsgaard, van der Sluijs, Brown, & van der Keur, 2006). The aim of expert elicitation is to gather knowledge from experts to make assumptions and assess variables and their uncertainties which is useful when creating conceptual models (Sebok et al., 2016). It is often used in multi-model simulations by asking different experts to provide conceptual interpretations and then comparing the resulting models.

To cover all uncertainties, including both sources and types of uncertainties, several methods should be used.

2.7.3 Sensitivity Analysis

To be able to identify parameter and model uncertainties in a complex model it can be beneficial to determine which parameter that are most influential on the model results (Hamby, 1994). This can be done by performing a sensitivity analysis (SA). There are

many different methods on how to perform an SA, however, generally it is conducted by the following steps, which is taken from Hamby (1994):

1. Defining the model and its independent and dependent variables.
2. Assigning probability density functions to each input parameter.
3. Generating an input matrix through an appropriate random sampling method, calculating an output vector.
4. Assessing the influences and relative importance of each input/output relationship.

A sensitivity analysis can be performed on a local or a global level. In a local SA, the analysis only addresses chosen parameters which entails that a sensitivity ranking can be obtained quite quickly by increasing the one chosen parameter at a time, with a given percentage, while the other parameters are set constant. Whereas, in a global SA, all parameters in the model are addressed.

Uncertainty and sensitivity analyses are often combined as a method to revise the model structure (Saltelli et al., 2006). The results of this process can sometimes lead to the conclusion that the inference of the many parameters in the model are too wide to be able to use the model as a basis for decision making. Although the model itself cannot be used in its solitude, the results of the analyses can strengthen the knowledge of which parameters that need additional research in the project, which would reduce output uncertainty in further revisions of the model. Sensitivity analysis is in some way a type of uncertainty analysis.

3

Case Study Application

This chapter contains a general description of the study area. Furthermore, it contains the conceptualisation of the site, structured on the basis of the framework for conceptual modelling in Table 2.1.

3.1 General Description of Case Study Area

The groundwater model is based on an aquifer system in a glaciofluvial deposit, *Umeälvsåsen*. This is located outside of Umeå municipality, in the county of Västerbotten, which is in the north part of Sweden along the east coast. The study area is part of Vännäs municipality, located approximately 30 km west of Umeå and includes several large rivers and valleys, which can be seen in Figure 3.1. The glaciofluvial deposit is an esker, called *Umeälvsåsen*. It follows the river, *Umeälven*, from north-west to south-east, and is one of the largest eskers in the area.

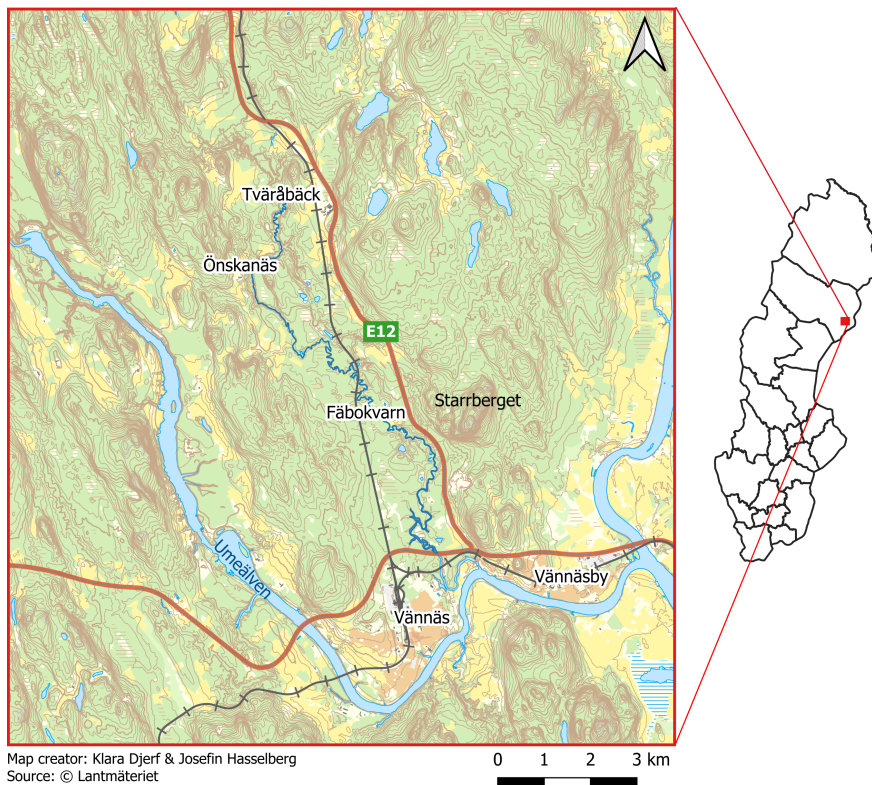
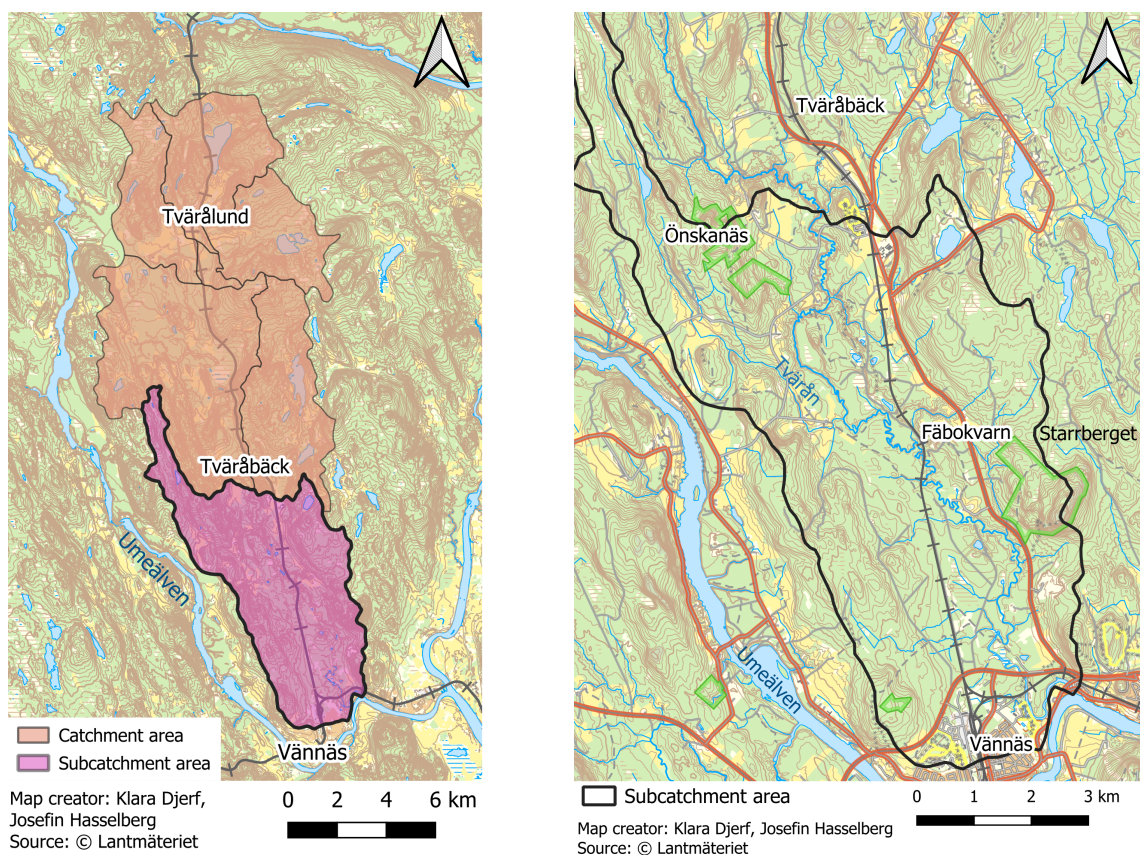


Figure 3.1: Overview map of case study area, located in Vännäs in the north of Sweden.

The land use in the area mainly consists of forest and some smaller areas of farmland. The area is sparsely populated. The esker is generally covered by forest, however, some gravel pits occur along the esker. Road E12 runs parallel to the esker on the eastern side and a railway runs along the area from north to south, crossing the esker between Önskanäs and Fäbodkvarn.

The topography in the study area is moderately hilly with some steeper slopes. Starrberget, with exposed bedrock, located east of the esker, stands out with a height of 150 m above the esker, which can be seen in Figure 3.1. In general, the area slopes towards southeast. On the east and west side of the esker, high elevation arises with exposed bedrock in some places. The area of interest in this thesis is located within a catchment area, presented in Figure 3.2.



(a) Map of catchment area.

(b) In-zoomed map of subcatchment area.

Figure 3.2: Overview map of the subcatchment area of *Umeälven* and the subcatchment area of *Tvärån*.

The catchment area of Umeälven is very large, stretching from the mountains in the north to a point located south of Vännäs. The case study area is located in one of the larger subcatchment areas of *Umeälven*, which is presented in Figure 3.2a. This catchment area is approximately 169 km^2 and of which 85 % consists of forest. The smaller subcatchment area of *Tvärån* is approximately 50 km^2 and its extent can be seen in Figure 3.2a and 3.2b. The higher altitude constitute the east and west boundaries of the subcatchment area. All of the surface water in the catchment area converges to a point in *Umeälven* in

the south of the study area. The river Tvärån flows through the area and crosses the esker south of *Fäbokvarn*. The average flow at the outlet to Umeälven is about $2 \text{ m}^3/\text{s}$. There are also some smaller water courses in the area that flow into Tvärån.

The geological, hydrological, and hydrogeological conditions of the site are partly known from earlier investigations from the 1980's and from Ramboll's investigations during 2018-2023. Some of the site data is available in a project report from Ramboll (Ramboll, 2022), such as measured stratigraphy and groundwater levels from boreholes/observation wells at different times. The assumptions and the data from the report have been used throughout the Case Study chapter. Furthermore, different types of maps of the project site, including soil maps and topography, are available from SGU (Geological Survey of Sweden) and Lantmäteriet (Land Survey). The hydrogeology in the area has also been studied by T. Wikner in two reports (Wikner et al., 2002a; Wikner, 2006), whose results will also be used in this chapter.

Furthermore, expert elicitation was used in the creation of the conceptual model. During a workshop with two hydrogeology experts, the geological model and its conditions were discussed, as well as boundary conditions of the model. The experts also contributed with assumptions and their "best guess" about parameter values and estimated data where essential information is missing.

3.2 Geology

Umeälvssäsen is located below the highest coastline, meaning that the glaciofluvial material was deposited below the shoreline during the last glacial period, Weichsel (10.000 years ago). A general stratigraphy of deposits below the highest coastline is presented in Table 3.1. Glaciofluvial material has been deposited in or just outside meltwater tunnels at the front of the ice sheet, during the retreat of the ice. The glaciofluvial deposits are often well-sorted with sand and gravel being the dominant grain sizes and have a high porosity and thus a high storativity. How well-sorted the material becomes is an effect of the fluvial processes, i.e. how much energy is present. Additionally, the grain size varies at different depths within a glaciofluvial deposit.

Table 3.1: Principle stratigraphy of deposits below the highest coastline.

Peat	Wind-	Wave-washed-	Young fluvial-	Postglacial deposits
		sediment		
		Clay (from transgression)		
		Wave-washed sediment		Glacial deposits
		Clay		
		Glaciofluvial sediment		
		Till		
		Bedrock		

A general cross-section of an esker, similar to Umeälvssäsen, is presented in Figure 3.3. The principal cross-section shows an esker in a valley with surrounding areas of till and exposed bedrock, which is very similar to the esker in the study area. The till typically extends from the outer areas with higher elevations and is sometimes beneath the esker at the edges. The cross-section shows that the glaciofluvial deposits contain coarse material such as sand, gravel, and stones. Above and on the side of the esker, fine-grained sediments

and silt-clay are deposited. Because of land rise due to glacial rebound deposits have been reworked in areas by wave erosion forming beach deposits on top of glacial till, fine-grained sediments and glaciofluvial deposits.

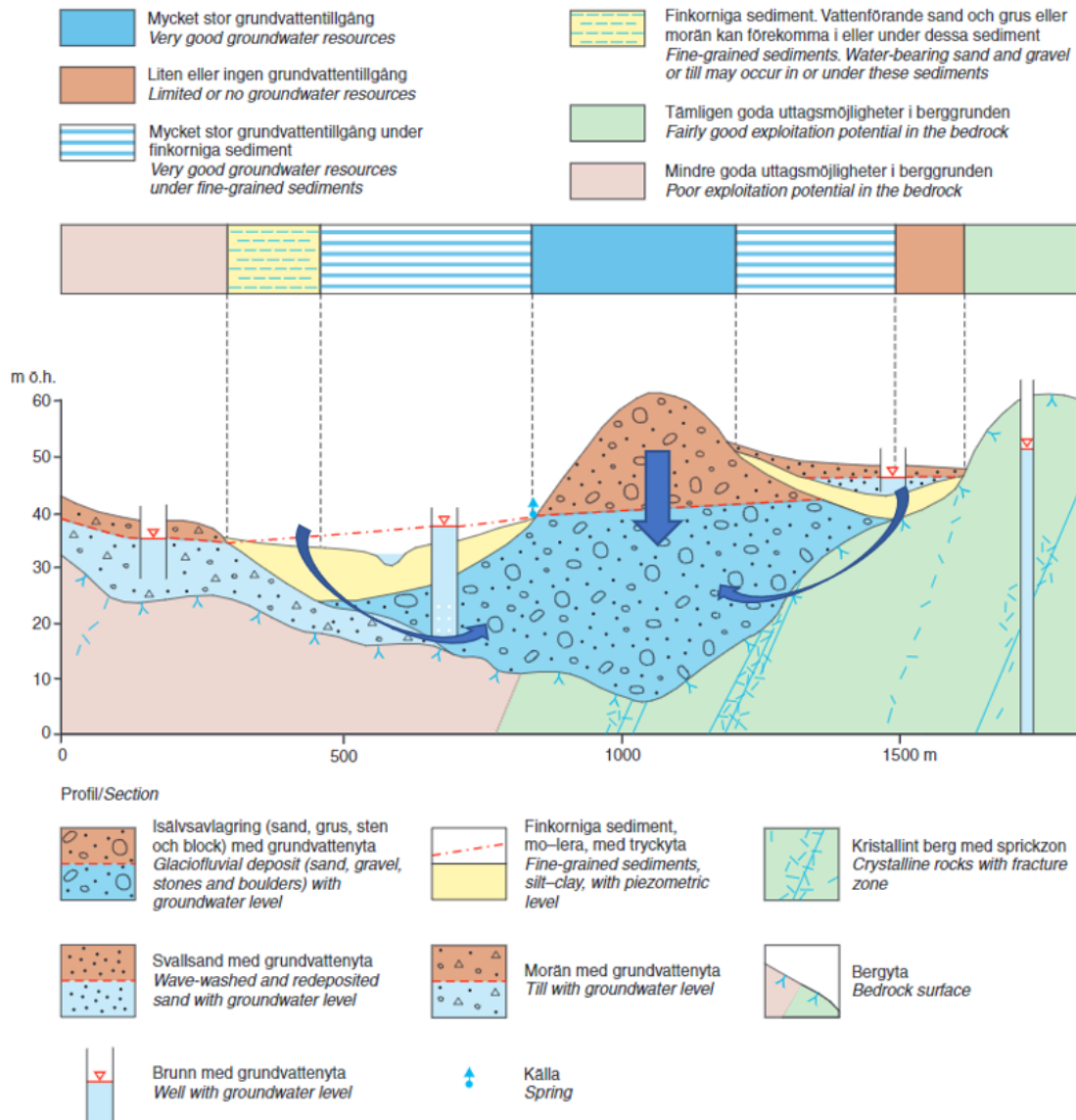


Figure 3.3: General illustration of groundwater in a glaciofluvial deposit, similar to Umeälvsåsen (Wikner et al., 2002a).

The soil type map from SGU illustrates the geology in the top layer of the study area and is presented in Figure 3.4. The esker is shown in green and stretches from north to south. The yellow area surrounding the esker represents fine materials, such as clay and silt. Small lakes and peat areas are present in conjunction with the esker, while till and exposed bedrock can be found at the edges of the catchment area. However, borehole data confirms that glaciofluvial material is overlain by finer materials as well. The esker is therefore larger than what is indicated on the map. According to (Wikner et al., 2002b), the esker is continuous from Bjurforsdammen to the study area, which is a total distance of approximately 15 km. In the subcatchment area, 10 km of the esker can

be found. Furthermore, the geological conditions imply that the aquifer is partly confined and partly unconfined.

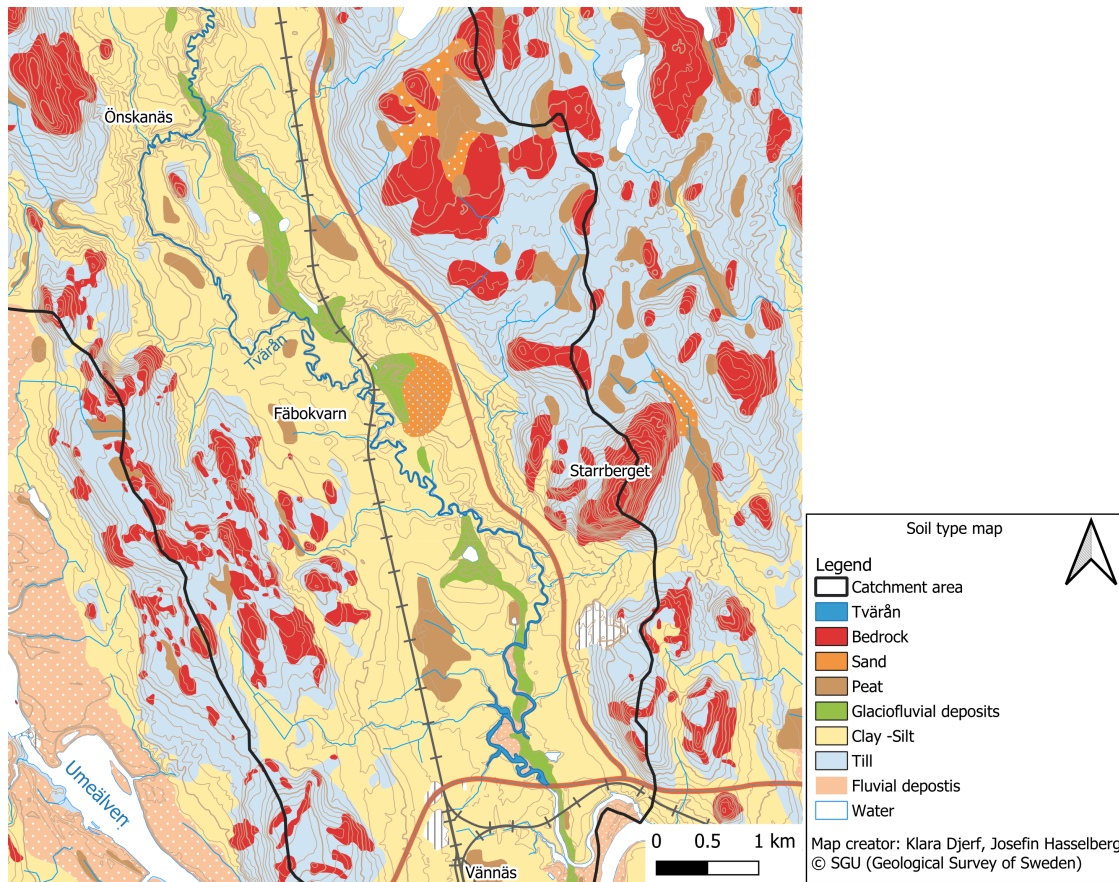


Figure 3.4: Soil type map from SGU over Umeälvsåsen and the subcatchment area.

Data from geotechnical investigations has been used to determine the soil and groundwater conditions. Drilling was carried out along the central parts of the esker to obtain information about soil type and layer sequence. Several boreholes are located along the esker but their specific location are not shown on maps due to secrecy. Soil type distributions at intervals of 1 m are available from each borehole. This data contains several different soil types from the field assessment. Geophysics were also employed in the central area of the esker to investigate the aquifer geometry and depth to bedrock. Seismic refraction is a geophysical technique that employs the refraction of seismic waves across soil layers and rock units to determine subsurface geological features (Green, 1974). Ground-penetrating radar (GPR) is another technique used to obtain an image of how radio waves reflect in the soil and rocks (Paz et al., 2017). The phase velocity of the wave provides information about soil layers and bedrock levels, as the phase velocity differs between soil types and saturation levels. Measurements were conducted both along and across the esker to evaluate the esker's geometry and layering sequence. However, no boreholes were located on the east and west sides of the esker. In these areas, the soil type map and knowledge about the general deposition of an esker have been used to develop the conceptual model, thus, the conceptual model is more uncertain in these areas.

3.3 Geological Model Development

The drilling results along the esker showed a highly variable sequence of layers within the study area. Thinner layers of fine materials were found in thick deposits of coarser materials. It is, however, necessary to simplify the geology in the model. Therefore, the experts at Ramboll simplified the model to only include five different soil types; fines, semi-fines, sand, gravel, and till. Semi-fines is assumed to be soil that is coarser than the fines but includes finer sediments than the sand and has therefore lower hydraulic conductivity. The simplification is based on the combined results from drilling and seismic analyses. The glaciofluvial deposits that form the aquifer, consist of gravel and sand.

In order to build 3D layers of the five different soil types, twelve profiles were created by the experts at Ramboll along the model area, where data from seismic investigations and boreholes were available. The profiles include topography and bedrock level, with soil layers created in between, which can be seen in Figure 3.5, where one of the profiles is presented. Since boreholes and seismic investigations were only available from the central parts of the esker, the outer areas of the profiles were based on professional judgement by Ramboll's experts. This is based on geological and hydrogeological knowledge, as well as knowledge about the depositional environment around an esker. According to the experts, the conceptualisation in the central part of the esker is, therefore, a good representation of the reality. The outer areas, however, are associated with large uncertainties about the stratigraphy and thickness.

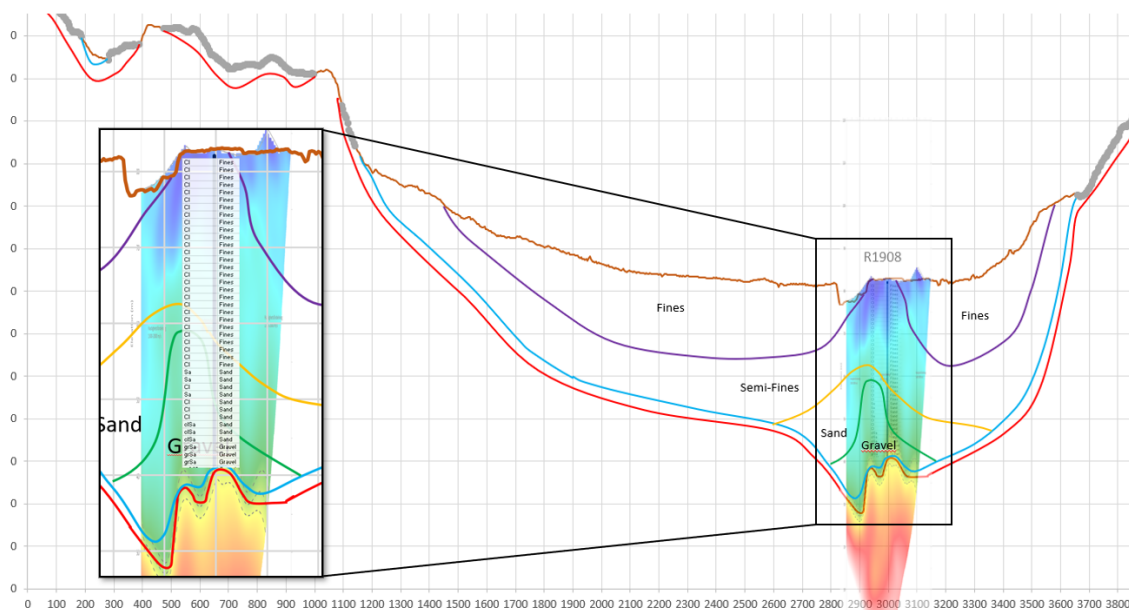


Figure 3.5: One cross-section profile of the esker, created based on knowledge about deposition environment, boreholes and seismic investigations. To the left, a zoomed in figure of how the borehole data and seismic result has been transferred to 5 different soil layers in the profile. The outer part of the profile is only based on knowledge about the geology in the area

The profiles were then imported into Leapfrog, which is a 3D geological modelling software that is designed to create and manipulate geological models using data, such as geological maps, borehole data, and geophysical surveys. The geological 3D layers were built by experts by importing the topography layer and the bedrock layer. To be able to define the bedrock as a layer, an additional horizontal layer were created as the base of the model, at level zero. Thereafter, the soil type layers were created and fitted to the profiles and then interpolated between the profiles, which can be seen in Figure 3.6. A cross section from the south part of the model can be seen in Figure 3.7.

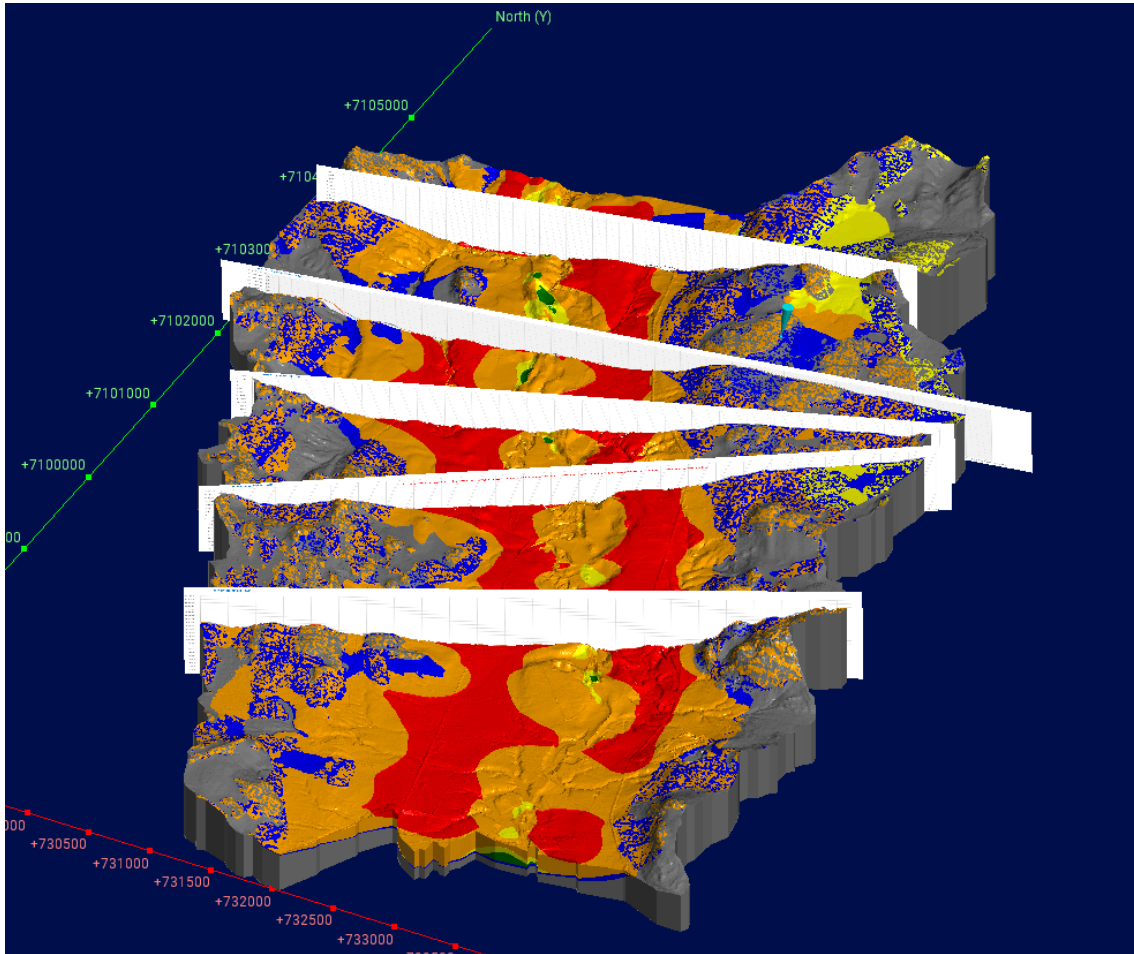


Figure 3.6: Geological model created in Leapfrog. Some of the profiles, which the model is created by, is shown as white lines crossing the model.

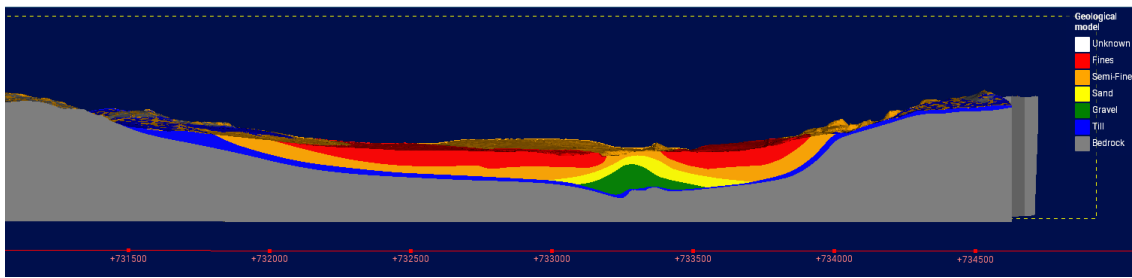


Figure 3.7: A cross-section of the geological model in Leapfrog from the south part of the area. Including a legend over the different soil types. The esker is clearly visible in the middle of the cross-section as the green/yellow ridge.

The cross-sections vary throughout the model with different thickness of the different soil types. Since the interpolation is made by a mathematical algorithm, layers had to be adjusted in a way that the experts found to be more natural and likely, based on the knowledge of glaciofluvial deposits. However, it is difficult to adjust the entire model with only 12 profiles in a model, which results in large uncertainties in the geological model.

In Figure 3.8, a cross-section is presented from the north-middle part of the model. The glaciofluvial materials, gravel and sand, has quite thin layers, whereas semi-fines has a very thick layer. Even further north, near the model boundary, there was no profile to interpolate to. This resulted in an unrealistic thickness of till, which can be seen in Figure 3.9. These uncertainties arise when the available data is not comprehensive over the esker, which is common in groundwater modelling.

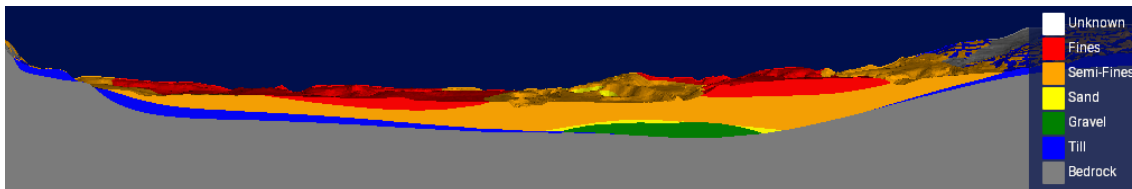


Figure 3.8: A cross-section of the geological model in Leapfrog from the north-middle part of the area. Including a legend over the different soil types. Showing a very thin layers of sand and gravel and a thick layer of semi-fines.

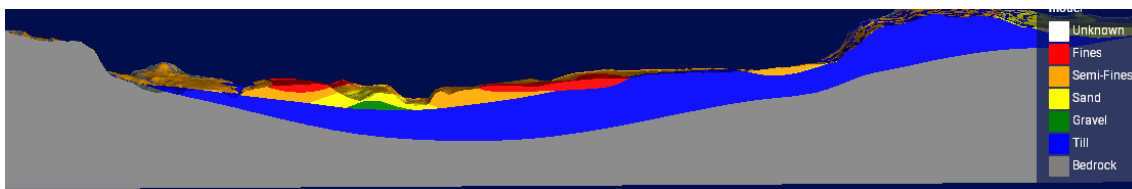


Figure 3.9: A cross-section of the geological model in Leapfrog from the north boundary of the area. Including a legend over the different soil types. Showing a very thick layer of till below the sand and gravel.

3.4 Model Area

When conceptualising the study area, a suitable solution was to employ the subcatchment area as the edges of the model area. Since the subcatchment boundaries align with the exposed bedrock, it forms a natural divide for groundwater flow, which gives the opportunity to define the east and west boundaries as no-flow boundaries. The north and south boundaries were cut according to Figure 3.10a since there are several benefits of having a smaller model area and since no-flow was not an option in these parts of the model due to the regional groundwater flow going from north to south. However, due to the interpolation errors with unrealistic thickness of till in the north and south part of the geological model, that was seen in Figure 3.9, it led to the model area being cropped. The final model area can be seen in Figure 3.10b.

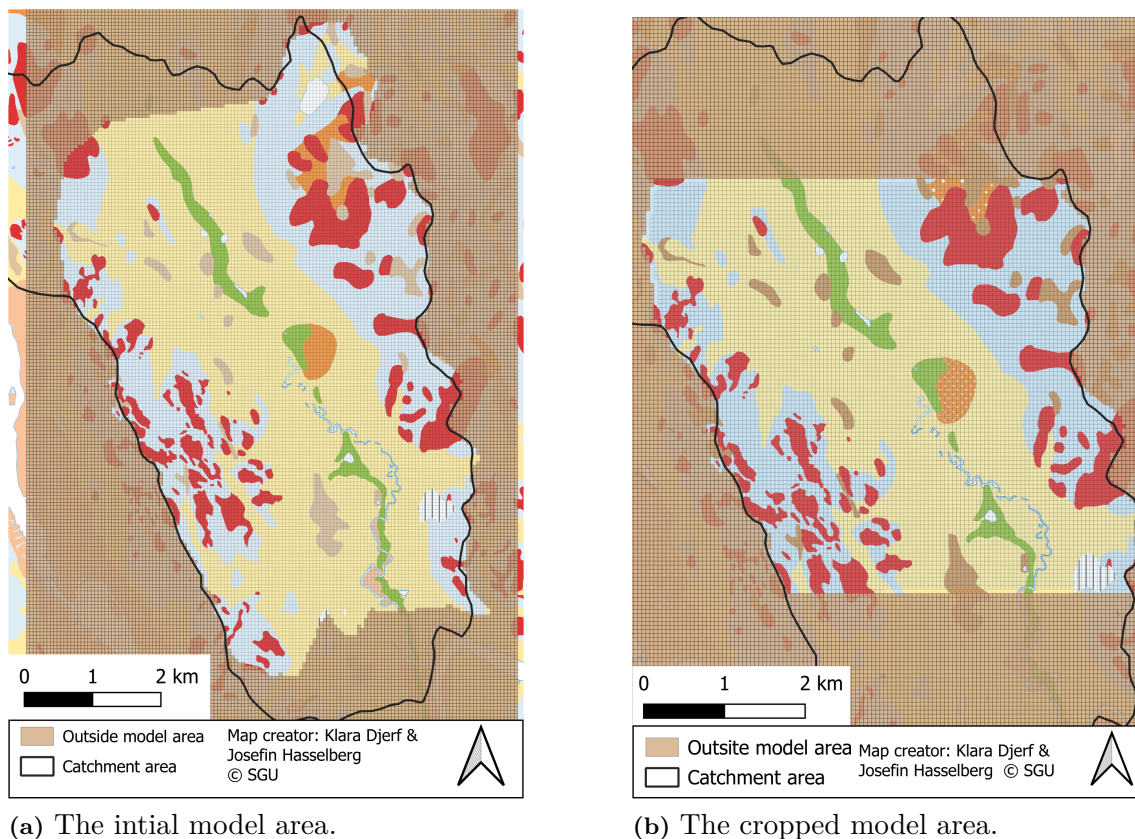


Figure 3.10: Overview map of the model area with the soil type map visual in the background. The model area is based on the catchment area.

3.5 Hydrogeology and Groundwater Recharge

Umeälsåsen continues further north from the case study area, following *Umeälven*. The esker comprises several aquifer systems and for the part of the esker located in the study area, there is a groundwater divide in Tvärålund, 12.5 km north of the area, which is visible in Figure 3.2a. In Önskanäs, just north of the study area, Vännäs municipality has their groundwater supply from the esker. The average pumping rate is $3000 \text{ m}^3/\text{d}$ (approximately 35 l/s). How the abstraction of groundwater affects the regional flow in the esker and the inflow to the study area is, however, somewhat uncertain.

Annual precipitation in the area is estimated to be ca 650 mm/year during measurements taken from SMHI (n.d.) from the period 1981-2010. When removing evapotranspiration from the precipitation, the annual net precipitation in the area is estimated to be 350 mm. The main part of the net precipitation recharges the groundwater (Wikner et al., 2002b). From observations in the area, it could be seen that there is a small amount of surface water runoff and only a minor portion of the net precipitation is subject to surface runoff.

Groundwater level measurements are available from observation wells located along the esker in the project area. Head data are available both from undisturbed conditions and from periods of long-term pumping tests, which have shown large volumes in the aquifer. The regional groundwater flow is assumed to account for a significant proportion of the groundwater volume in the project area. However, due to a lack of monitoring points on the sides of the esker, the ratio between how large volumes comes from the inflow and the volume of water that comes from recharge in the entire sub-catchment area is uncertain.

The recharge of groundwater in the esker depends on how the esker was deposited and its connection to other soil layers. Furthermore, recharge also depends on the slope of the ground in less permeable soils, since a steeper slope leads to more surface runoff in clay or exposed bedrock. Since the pumping tests, that were conducted, showed great abstraction capacity, it indicates a high groundwater recharge in the area. Based on pumping data and geological information about the site, the till and bedrock areas in the outer parts of the catchment area most likely act as recharge zones for the esker, see Figure 3.3. The recharge area is considered to be extensive and its outer boundary is assumed to coincide with the catchment area, that is presented in Figure 3.2b. The groundwater recharge is assumed to be high where the glaciofluvial deposits reaches the ground level and it is probable that most of the net precipitation infiltrates there. In coarse-grained till areas, the recharge is possibly around 200-250 mm/year, but in areas with fine materials the recharge could be as low as 50-100 mm/year. In Figure 3.11, the catchment area is presented together with arrows, illustrating the assumed groundwater flow directions. The large arrow from the north illustrates the regional flow in the esker. In addition, the figure illustrates the important groundwater recharge from the areas of till.

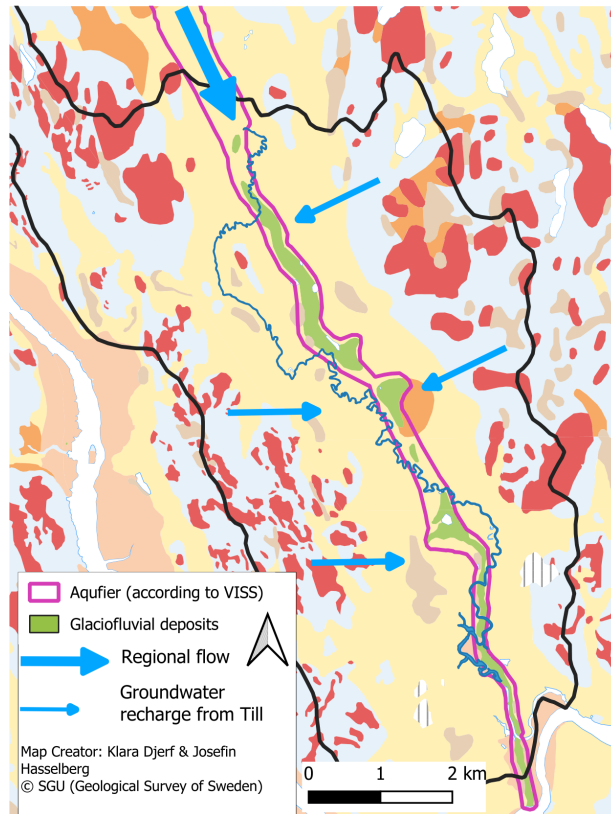


Figure 3.11: Map over catchment area with illustrations of the groundwater flow directions. Including a legend describing the different arrows and colours in the map.

The amount of recharge that occurs in different soil types depends on their hydraulic conductivity, which is the measure of how easily water can flow through the material per time unit [m/s]. Hydraulic conductivity (K-value) differs between the different soil types depending on grain size distribution and how well sorted a material is. A well sorted material has smaller pores, however, since the particles are of similar size and shape, it reduces the number of pathways that water can take through the material. This results in higher hydraulic conductivity. Glaciofluvial deposits has a high K-value, and typically a high groundwater flow, whereas materials such as silt and clay has very low K-values and thus low permeability. Measurements of hydraulic conductivity usually presents an average value of conductivity for all directions in the material. However, for finer materials deposited in layers, the horizontal conductivity (K_h) are usually higher than the vertical conductivity (K_v). Thus, K in different directions is highly dependant on grain size and the structure of the material. For example, K_v in clay could be assumed to be 10 times less than K_h in some areas.

In order to create a flow throughout the model, it is essential to use realistic values of hydraulic conductivity (K-values) in the different soil type layers. Therefore, K-values for sand and gravel were taken from Ramboll's observation well data. As presented in Figure 3.12, all the observation wells were located along the esker, which resulted in a large amount of hydraulic conductivity data in gravel and sand, but no data for the surrounding soil types. However, the observation wells are quite scattered along the esker,

which gives a good representation of the glaciofluvial K-values.



Figure 3.12: Observation wells located in the model area. All observation wells are located along the esker. The orange polygons illustrating the division of observation wells in three zones.

When calibrating the model to be as close to reality as possible, it is beneficial to have an interval of K-values for the different soil types. When reviewing the values in a histogram, which is presented in Figure 3.13, it was clear that some outliers were present in both sand and gravel. Furthermore, it is visible that hydraulic conductivity for gravel varied greatly from different boreholes and depths, thus the standard deviation (*stdev*) curves in Figure 3.14 overlaps. To be get a useful interval for gravel and sand, the maximum K-value for sand and gravel were then calculated by taking $mean + (stdev \cdot 2)$. For sand, the minimum value used in the interval was the same as the minimum measured value. Whereas, for gravel, the smallest measured values that were below the smallest values for sand, was removed in order to get a more reasonable interval. This is considered to the assumption that gravel is more permeable than sand.

When assigning hydraulic conductivity intervals for the remaining soil types, some assumptions had to be made with help from the experts. In Table 3.2, the intervals for all soil types in the model are presented. The minimum and maximum K-values were assumed by the experts at Ramboll for fines, semi-fines, and till. K-values for bedrock were taken from SGU (n.d.), where hydraulic conductivity has been defined in different parts of the study area. The arithmetic mean value was then calculated from the minimum and

maximum values for all the soil types.

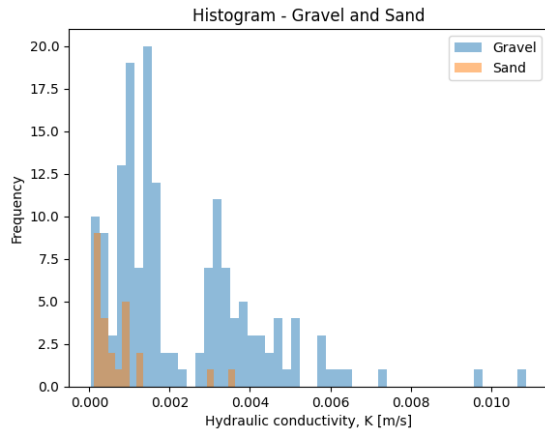


Figure 3.13: Histogram of hydraulic conductivity values of gravel and sand.

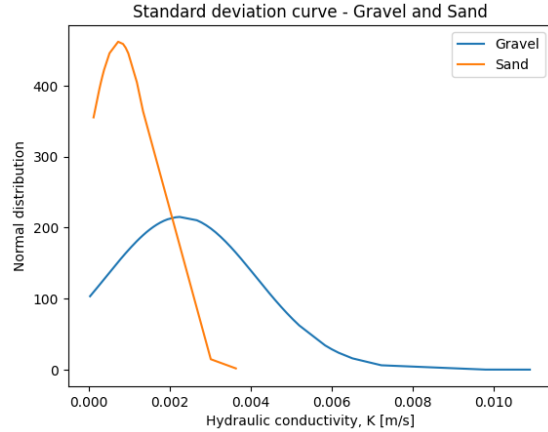


Figure 3.14: Normal distribution of hydraulic conductivity of gravel and sand.

Table 3.2: Hydraulic conductivity minimum, maximum, and mean, for all soil types.

Soil type	Min [m/d]	Mean [m/d]	Max [m/d]
Fines	0.001	0.044	0.086
Semi-fines	0.864	22.032	43.200
Sand	10.022	60.555	111.088
Gravel	16.934	268.364	519.793
Till	0.043	0.454	0.864
Bedrock	0.009	0.048	0.086

3.6 Boundary Conditions

This section presents what type of boundary conditions that was defined on the edges, and within, the model area and where they are present. Four different types of boundary conditions are used and is presented in Tabel 3.3.

Table 3.3: Boundary conditions.

Boundary condition	Description
Flow Boundary	The flow through the boundary is specified to a specific value.
Head-Dependent Boundary (General Head)	The groundwater level (head) is specified as a reference head at the boundary and flow through the cell vary in the model depending on the simulated level compared to the reference head.
Specified Head Boundary	The groundwater level (head) is set to a specified value at the boundary.
Head-Dependent Flux Boundary (Drainage)	The boundary drain water from the model if the simulated head is higher than a reference head that is specified at the boundary. The water can only leave the model through the drain and not re-enter.

3.6.1 Boundary Conditions along the Edges of the Model Area

Figure 3.15 presents boundary conditions along the edges of the model domain that are not defined as no-flow boundaries. Depending on assumed hydraulic conditions, the flow boundary has been divided into three sections; Boundary condition A, B, and C.

The section with Boundary condition A is located where the regional inflow is assumed to flow and Boundary condition B is where the outflow from the model is. Both section A and B can be defined with a flow boundary where a specified flow is set as an input value. Considering the shape of the esker and the measured groundwater levels in the project area, it is assumed, by experts at Ramboll, that the total inflow from the north is ca 75-125 l/s and the total outflow in the south is ca 175-275 l/s . The inflow and outflow is then distributed unevenly in the flow boundary cells so that most of the groundwater flows in the glaciofluvial materials, especially in the gravel, which has the highest K-value. It is also possible to use a head-dependant or a specified head boundary in section A and B. The inflow and outflow is then computed to satisfy the water balance in the model.

Boundary condition C cells are located in the top left corner of the active area, as well as on the right side of the flow boundary cells, in cells where till is surfaced. These cells are chosen as an assumption that the water table is commonly located 1-2 m below the ground in till. Thus, it is possible to use a specified head or a head-dependent boundary defined as 1.5 m below the surface for these cells.

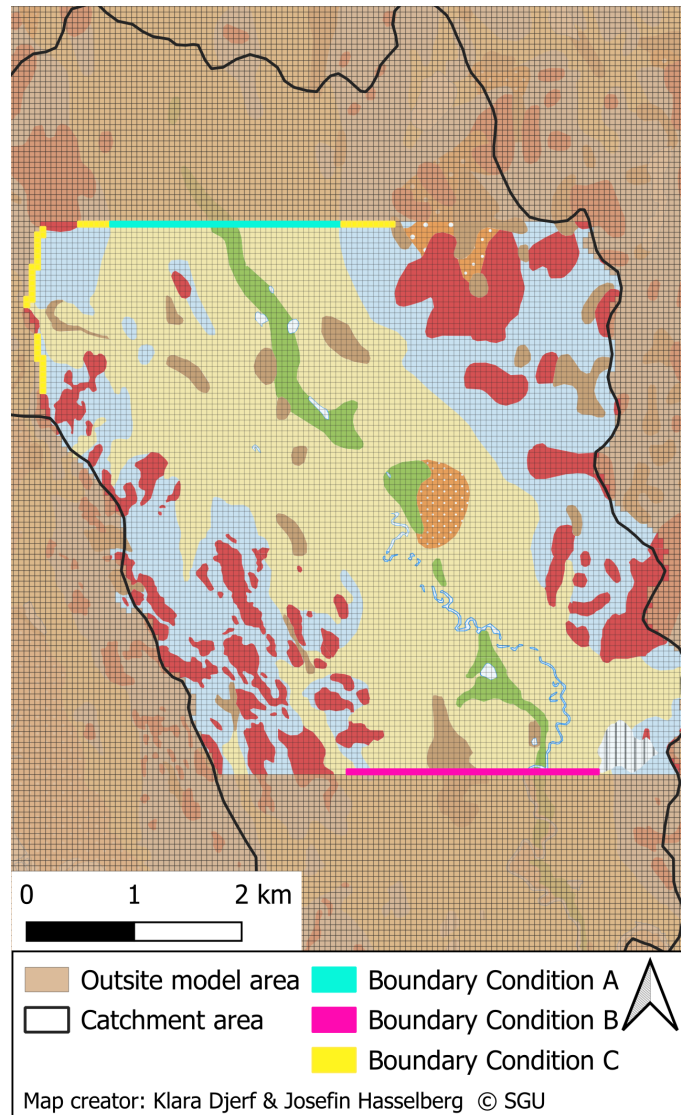


Figure 3.15: Locations of boundary conditions within the model area. Including a legend presenting different boundary conditions and the model area. The boundary conditions are located at the edges of the model area, in three sections named A, B, and C.

3.6.2 Boundary Conditions within the Model Area

As mentioned in Section 3.1 General Description of Case Study Area, there is a stream in the area, called Tvärån. It is somewhat unknown if there is a strong correlation between the stream and the aquifer, however, it is possible that there is a significant connection between them that could influence the hydraulic properties of the aquifer. Where Tvärån crosses the esker, the glaciofluvial deposits is in direct contact with the surface water, which can be seen in Figure 3.11. During field visits, groundwater discharge was visible at *Fäbokvarn*, which is located where Tvärån crosses the esker. It can therefore be assumed that no surface water flow into the esker in that part of the area. In other areas, a connection between the stream and the aquifer is likely to be limited due to the presence of fine material. Nevertheless, it is necessary to investigate it further to verify a connection.

The possible impact from Tvärån on the aquifer can be seen as an additional boundary

condition in the model and can be categorised as a head-dependent flux boundary which is a drainage. Figure 3.16 presents Tvärån as Boundary condition D and where it is located in the model domain. The drainage was implemented along the entire Tvärån because it is uncertain how the river cuts through the clay sediments.

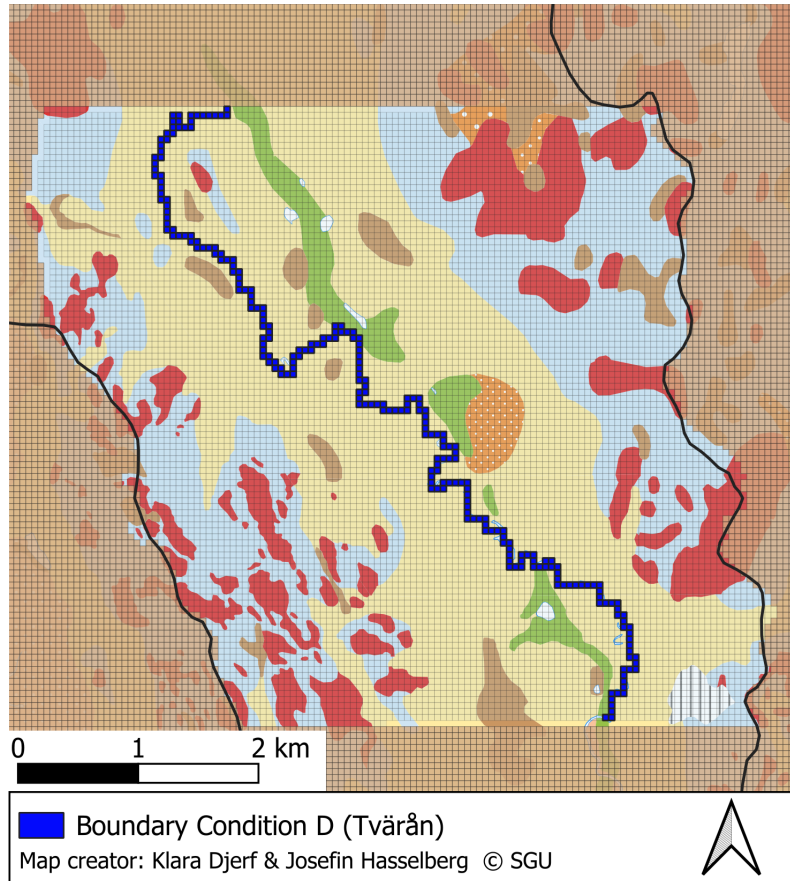


Figure 3.16: The location of Boundary condition D illustrating the river Tvärån in the model area. The Boundary condition D going through the whole model area from north-south.

Furthermore, the area contains several smaller ponds. However, groundwater measurements in the esker compared to the surface water level indicates no clear connection between the smaller ponds and the aquifer. This assumption is partly based on the presence of more impermeable underlying materials, which suggest a lower potential for fluid flow or transport.

3.7 Multiple Groundwater Models

In order to meet the aim of the study, a number of different models were created. Table 3.4 presents 12 models and which boundary conditions that was used along the model domain boundary (in A, B, and C) and if the stream, Tvärån, was draining the area or not (Boundary condition D). The models are named according to the structure of Model ABC-D, using the following conventions: F for flow boundary, S for specific head, G for general head, D for drain, and ND for no drain. The first six models has all different

boundary conditions and the drain included. The last six models has the same boundary conditions for A, B and C as the first six but no drain (D) included.

Table 3.4: All groundwater models with different boundary conditions and their names.

Models	Boundary condition A (North)	Boundary condition B (South)	Boundary condition C (Till cells)	Boundary condition D (Tvärån)
Model FFS-D	Flow Boundary	Flow Boundary	Specified Head	Drain
Model SFS-D	Specified Head	Flow Boundary	Specified Head	Drain
Model FSS-D	Flow Boundary	Specified Head	Specified Head	Drain
Model SSS-D	Specified Head	Specified Head	Specified Head	Drain
Model GGG-D	General Head	General Head	General Head	Drain
Model FFG-D	Flow Boundary	Flow Boundary	General Head	Drain
Model FFS-ND	Flow Boundary	Flow Boundary	Specified Head	NO
Model SFS-ND	Specified Head	Flow Boundary	Specified Head	NO
Model FSS-ND	Flow Boundary	Specified Head	Specified Head	NO
Model SSS-ND	Specified Head	Specified Head	Specified Head	NO
Model GGG-ND	General Head	General Head	General Head	NO
Model FFG-ND	Flow Boundary	Flow Boundary	General Head	NO

4

Numerical Model Development

To build the numerical model with MODFLOW, using Flopy, the steps in section 2.5 MODFLOW were followed. There are various versions of MODFLOW available for defining and running a MODFLOW model, including MODFLOW-2005, MODFLOW-NWT, and MODFLOW 6, where MODFLOW 6 is the latest version. Available material, such as tutorials and notebooks, which were necessary for the model building, were available to the greatest extent for MODFLOW-2005. Additionally, an online guide to MODFLOW-2005 is available from the developer, (USGS, 2022). Therefore, MODFLOW-2005 was chosen to be used. It was necessary to install and import usepackages and libraries into the Python code to build the model script. The libraries NumPy, Matplotlib, SciPy, and Pandas, were installed as well as the packages; FloPy, Shapely, and Fiona. In the script, packages from the flopy.modflow-module were used to import data into the model (USGS, 2022). Each package used from the flopy.modflow-module includes several parameters. Some parameters have been manually assigned and are presented in this chapter, while others are kept as their default values and are not presented. The numerical model development is further explained in this chapter. The script can be found in Appendix B.

4.1 Discretisation

To transfer geological information from Leapfrog to the numerical model in Python, a MODFLOW model was exported directly from Leapfrog. The model contained several files, including a .nam-file, which is the actual model, and a .dis-file, containing information about discretisation, which is the input file for the DIS package. The dis-file contained a square-shaped grid that spanned the x-y plane, where each cell had dimensions of 50 x 50 meters. In Flopy, the model is represented as a grid with 240 rows (y-axis), 144 columns (x-axis), and 5 layers (z-axis), where each position in the grid is one cell. To define properties for certain cells, they are defined by their location in the grid as [layer, row, column]. The DIS package also contains information about the simulation stress period and whether the stress period is steady-state or transient. The stress period is defined as one day, and the model is run as steady-state, meaning that the model is considered to have reached a steady state and parameters are set as constant throughout the simulation.

The bas-file was also included in the MODFLOW model from Leapfrog, which is the input file for the BAS package, a required package for all MODFLOW models. The BAS package includes information about active/inactive cells and starting heads. The *ibound* parameter defines the cells as active (1), inactive (0), and an active cell with specified head (-1). Starting heads are the head in each cell at the beginning of the simulation and is defined with the *strt* parameter. The starting head has a significant influence on the water

balance, since it affects the amount of water in the model. To allocate these properties to each cell, the MODFLOW model was exported as a shapefile to the geographic information system, QGIS. QGIS was used to visualize the model and locate where specific conditions should be placed, based on the soil type map from SGU. In QGIS, it was easy to work with the grid and assign different values to different cells in the attribute table. The data were then exported from QGIS as a .csv-file and loaded into the script. From a .csv-file, it is possible to create an array, which is a way to store data in Python, which can be included in MODFLOW packages.

4.2 Geology

The model contains six different soil types, as can be seen in Figure 3.7. However, the layers in the z-axis are not reconciled with the soil types, which is visible in Figure 4.1. The cross section of the Leapfrog model is presented with the grid where each bar represents the columns and the horizontal lines represent the layer boundaries. In the right part of the figure, one column with 5 cells is presented, which shows how one soil type could be fitted into several layers to capture the right thickness of the material in the model. Information about which soil type each cell has in the MODFLOW-model was stored in a .zon-file in the export from Leapfrog. In Python, the .zon-file was read and an array was created with the same size as the grid with indicators of 2-7 representing all soil types, (2 = Fines, 3 = Semi-Fines, 4 = Sand, 5 = Gravel, 6 = Till, 7 = Bedrock). This array provides opportunities to assign different values to different cells based on the soil type.

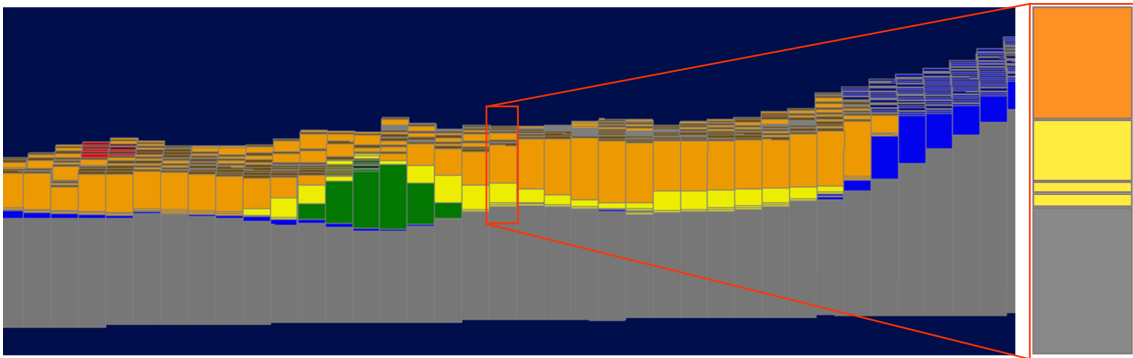


Figure 4.1: A Cross-section of the Leapfrog model with the grid and soil layers visible. To the right a zoomed-in column from the grid illustrating that the same soil type is assigned to several layers in the model.

4.3 Hydrogeology and Groundwater Recharge

The Layer-Property Flow package (LPF) defines hydraulic conductivity, which controls flow between cells. The horizontal hydraulic conductivity is specified using the hk parameter, which is assigned to each cell based on its soil type. Additionally, the hk parameter is divided into three zones - North, Middle, and South - to allow for different K-values to be assigned for each soil type throughout the model. The vertical hydraulic conductivity, vk , is assigned in the same way as hk .

Recharge is defined in the Recharge Package (RCH), which simulates precipitation on the top layer in the model. MODFLOW calculates the flux of recharge based on the cell area and recharge per unit time and length (m/d). The effective precipitation is used as the recharge.

4.4 Boundary Conditions

The four boundary conditions A, B, C, and D, are specified by three different packages in the model. The boundary condition locations in the model are presented in Figure 4.2, where active and inactive cells are also shown. To decide which cells should be assigned different boundary conditions, QGIS was used, and the cell locations (layer, row, column) were exported to Python.

The Flow and Head Boundary Package (FHB) is used for specified head and specified flow cells, which is used in all models except for Models GGG-D and GGG-ND. In the package, the parameters *nhed* (number of cells with specific head) and *nflw* (number of cells with specific flow) vary between the models depending on the boundary conditions and their location. Specific head is assigned in cells in the top layer, and specific flow is assigned in cells in all layers where the boundary conditions are located. The data set parameters *ds5* and *ds7* define the specified cells and their constant head and flow values. Where specific head is defined, the *Ibound* parameter in the BAS package is set to -1 to make the cell a specified head cell.

The General-Head boundary package (GHB) is another boundary package used to simulate head-dependent boundaries. GHB is used in models GGG-D, FFG-D, GGG-ND, and FFG-ND as a general head. The only parameter defined in the package was *stress;period;data*, where the general head cells are defined, as well as their *stage* and *cond* values. GHB is used for Boundary Conditions A, B, and C.

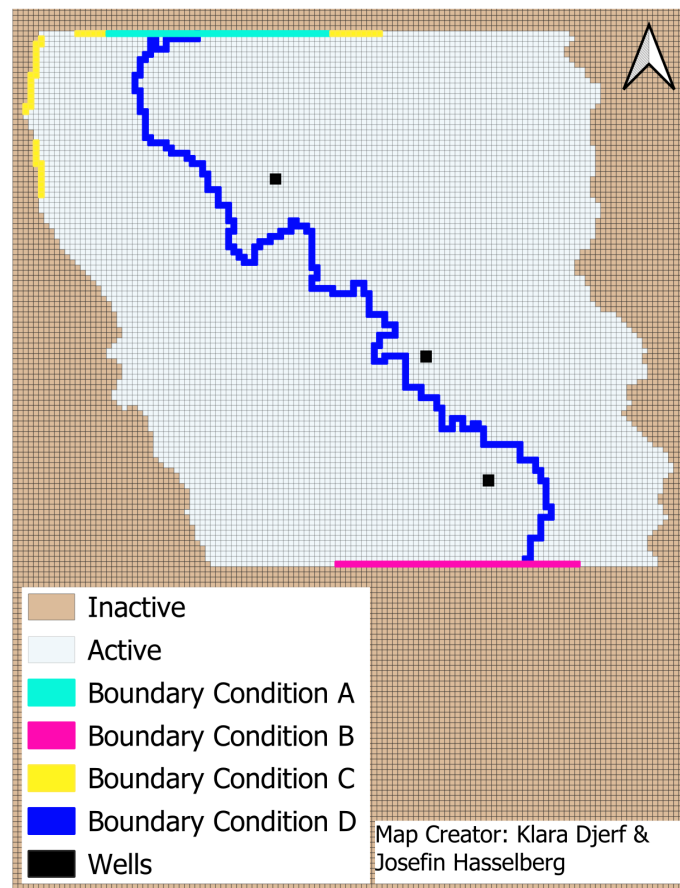


Figure 4.2: Conceptualisation of numerical model and location of different boundary conditions A,B, C, and D. Illustrated in QGIS. The legend is showing the colours for different boundary conditions, active and inactive cells, and the pumping wells.

For Boundary Condition D, the Drain Package (DRN) is used to simulate possible drainage from Tvärån. The drain package, like the GHB, is a head-dependent flux boundary. Each drain cell is defined in the *stress;period;data* parameter, where its location, *stage*, and *cond* values are specified. The *stage* for the drain is set to 1 m below the top elevation in each cell. The *cond* parameter is the conductance (m^2/d) in the river and is defined as the hydraulic conductivity in the riverbed sediments multiplied by the area of the river in the cell. The DRN package is used in the first 6 models, which all include drain.

4.5 Pumping

To simulate the model's response to a pumping event, the well package (WEL) is used. Three wells were placed at three different cells in the model, where actual pumping tests has been performed. The location of these wells can be seen in Figure 4.2. The flux and location of the well are defined in a *stress;period;data* package within the WEL package. The pumping is assigned to layer 3 (number 2 in Python, since it is starting from 0), which is in the middle of the esker. The flux that is used is the same as the actual pumping test: 55 l/s in the north, 45 l/s in the middle, and 75 l/s in the south.

4.6 Model Run

The output control package (OC) controls which outputs that will be saved in the simulation. In the package it is specified that the output will be saved at the end of the stress period and that head and water budget will be printed and saved. To be able to run the model, a solver needs to be added. The Preconditioned Conjugate-Gradient Package (PCG-Solver) was used as it is the most common solver to use in order to solve the finite difference equations in a MODFLOW simulation. The last step before running the model is to write input files based on all packages included. When all input files are ready, the model can be run by Flopy using an executable file (mf2005.exe).

4.7 Calibration

After running the model, all hydrogeological parameters were manually calibrated. The purpose of calibration is to determine the most appropriate parameter values for the model setup. Since all parameters affect the water balance in the model, calibration was done as an iterative process, running the models over and over again, to find the best combination. The simulated heads in the model were compared with observed heads from observation wells, and the cross-sections with heads along the esker were studied to understand how the model worked and what the levels looked like.

Two approaches were tested for determining the starting head, represented by the *strt* parameter: (1) assuming the levels were 1 meter below the ground surface, and (2) interpolating groundwater levels based on levels in observation wells. To interpolate the layer, three steps were taken. First, levels were interpolated from measured values in observation wells in the central part of the esker. Secondly, on the sides of the aquifer up to the outer edges, the levels were set to 1 m below the ground surface. Thirdly, in the interface between the interpolation from observation wells and the outer areas, another interpolation was made to smooth out the levels.

The span of K-values, presented in Table 3.2, were manually calibrated by testing different combinations within the interval. As mentioned in Section 3.3 Geological Model Development, there are some cross-sections in the geological model with very thin layers of sand and gravel and large thicknesses of Semi-Fines. Therefore, higher K-values for Semi-Fines were tested outside the interval to resemble the glaciofluvial deposits and ensure regional flow from north to south. Two approaches were tested in order to determine the K-values : (1) the same K-values for each soil type within the entire model and (2) dividing the model area into three K-value zones; north, middle, and south, and assigning different K-values for each soil type in the three zones. The values were then taken from boreholes and divided according to Figure 3.12.

Recharge was calibrated by changing the percentages of recharge in different soil types in the top layer. The amount of recharge in sand and gravel was set to 100 % = 350 mm/year. For the other soil types, different percentages were tested based on the conceptualisation that less recharge occurs in fines and bedrock but that the till contributes to recharge to a larger extent. Additionally, this also led to less recharge in the outer areas where steeper slopes are present.

Furthermore, inflow and outflow in the FHB package were tested within the range mentioned in Section 3.6.1 Boundary Conditions along the Edges of the Model Area and with a different share of the flow in different soil types. The total flow in each material was

then divided by the number of cells with each soil type that was present in the boundary. In addition, where specified head was defined in Boundary condition A and B, the head was calibrated and changed along the boundaries to find a head that was consistent with the starting head.

According to an experienced groundwater modeller at Ramboll, conductance is a difficult parameter to calculate based on equations. A common approach is, therefore, to test different values to see the model's response. The calibration started at $8640 \text{ m}^2/\text{day}$ and was then changed by a factor of 10 in both directions in the drain package. The *cond* parameter in GHB package, was set to 10 times larger than the *hk*-value for each soil type.

4.8 Multiple Groundwater Models

When the calibration is done and the most suitable combination of parameter values were found for the model, the model is ready for different simulations. Multiple groundwater models are then created with different boundary conditions, as described in 2.1, to simulate the model response with changes in the system. To further evaluate the model, one pumping event were performed for each model.

4.9 Result Analysis

To analyse the results, the groundwater heads are saved and plotted in different ways. Cross-sections throughout the models are plotted to illustrate the groundwater level within the model and how the levels appear in relation to the topography. Head contours are plotted to visualise the head levels throughout the model, which is visualised with an overhead view. Simulated values in observation wells were studied and compared with observed values. Lastly, the water balance for the model, showing how much water going into the model and how much going out, were studied. The balance should be as close to zero as possible. Water going into the model comes from recharge, specified inflow and specified head. Water that is going out of the model is specified outflow, drainage and specific head. When assigning specified or general head as a boundary condition, the natural gradient will determine whether it is flowing in or out of the model.

Since several models are studied, a sensitivity analysis is made. The heads in the different models are compared both to the observed head values, as well as to each other. This is done in order to investigate if all the models are feasible options and to determine how the boundary condition options affect the model results.

5

Results

This chapter presents the results from the modelling process and from the different models. After calibrating the models, values for all hydrogeological parameters were set. The parameter values that were used in the models are presented in Appendix A.

Note: The model names are based on the boundary conditions A (north), B (south), C (till cells), and D (drainage). The models are named according to the structure of Model ABC-D, using the following conventions: F for flow boundary, S for specific head, G for general head, D for drain, and ND for no drain.

Figure 5.1 presents simulated head from all models and compares them with the observed head, that was earlier measured in several observation wells located throughout the model area. Observation well R2207 has an abnormal observed value, which could be due to its location on the side of the esker compared to the other observation wells. Therefore, this value could be somewhat disregarded. The result shows that all models with a drain have significantly lower head than the models without a drain. The models with a drain follow the observed values in the middle and south part of the model (to the right in the figure). In the south, the head of Models FFS-D, SFS-D, and FFG-D clearly positively correlates to each other, as well as Models FSS-D, SSS-D, and GGG-D. Moreover, the simulated head values are higher in the north part (to the left in the figure) for all models. The largest difference between the models with and without a drain is in the north section.

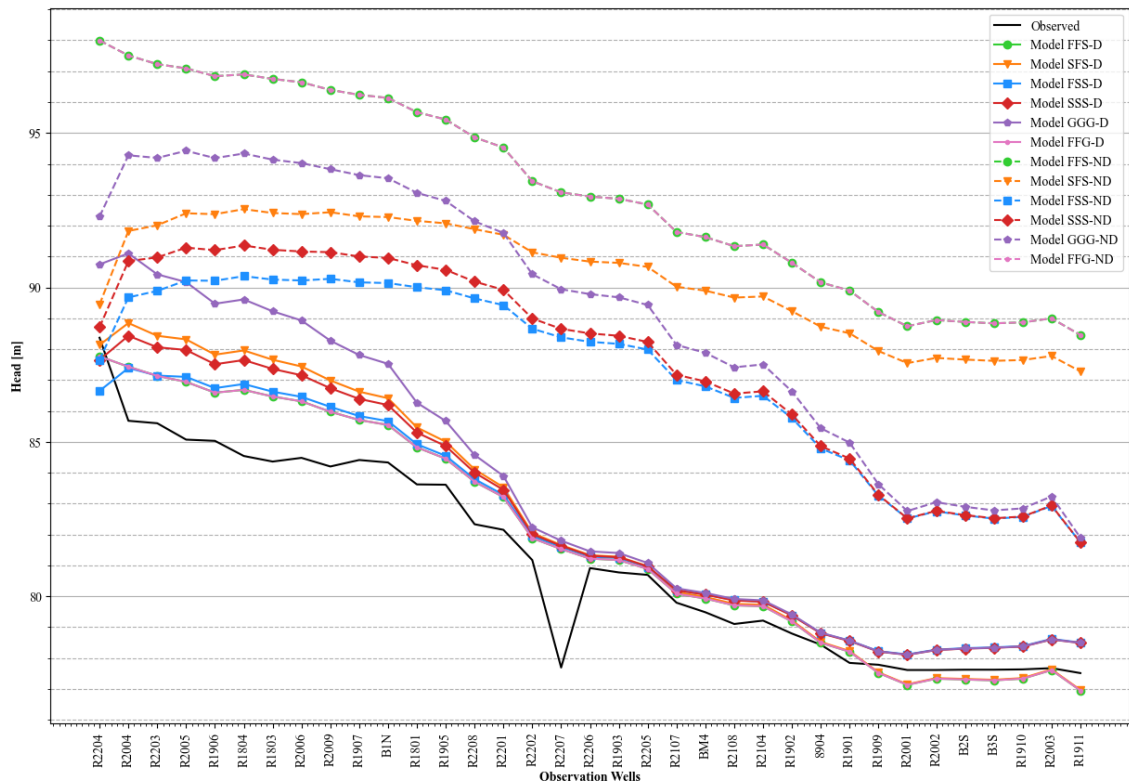


Figure 5.1: Simulated head from all 12 models plotted together with observed head in several observation wells from north to south in the model area. Observed values are marked with a black line and the models with the same boundary conditions are colour matched. All models with drain has solid lines and those without drain has dashed lines.

The groundwater level (head) in relation to the topography is presented in Figure 5.2 and Figure 5.3, which displays three cross-sections for Models FSS-D and FFS-ND. Model FSS-D exhibits head levels that closely resembles the observed ones. The model features a flow boundary in the north, where the groundwater level is a few meters below the ground surface, specifically where the esker is located (in the middle of the cross-section), which is presented in Figure 5.2a. Towards the sides, the head is higher and generally follows the topography, which is similar to the starting head in these areas. Elevated groundwater levels are visible on the sides in all cross-sections. Figure 5.2c showcases the south boundary, where a specified head is present and indicated by blue columns, resulting in high head levels in this region.

Figure 5.3, on the other hand, shows cross-sections from one of the models without drainage, where it is clear that the levels are higher throughout the model area compared to the levels in Figure 5.2. Model FFS-ND, has groundwater levels several meters above the ground surface in all three cross-sections.

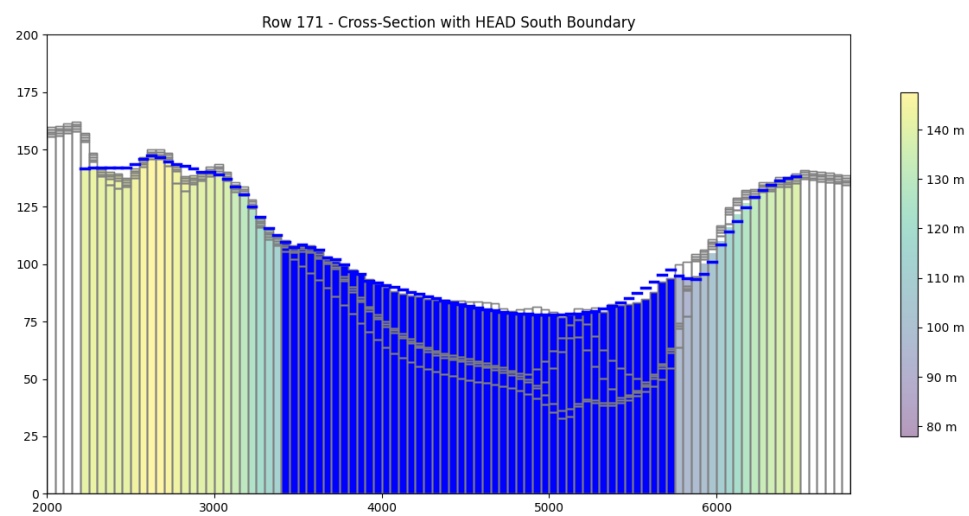
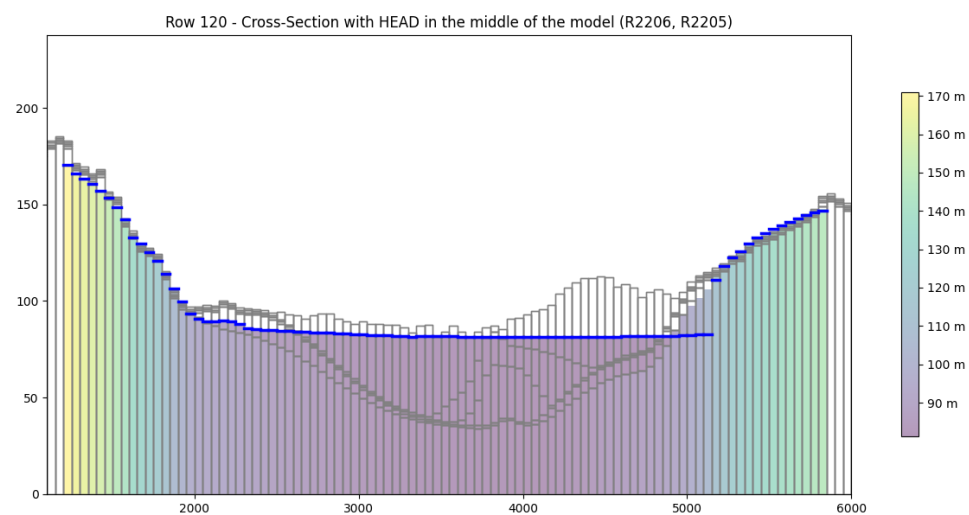
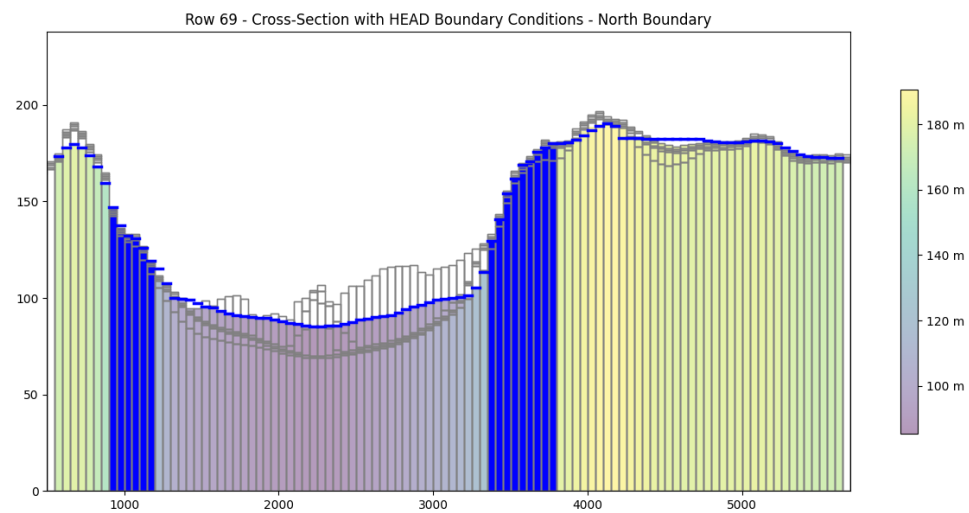


Figure 5.2: Cross-sections (west-east) of model SFS-D at three different locations in the model.

5. Results

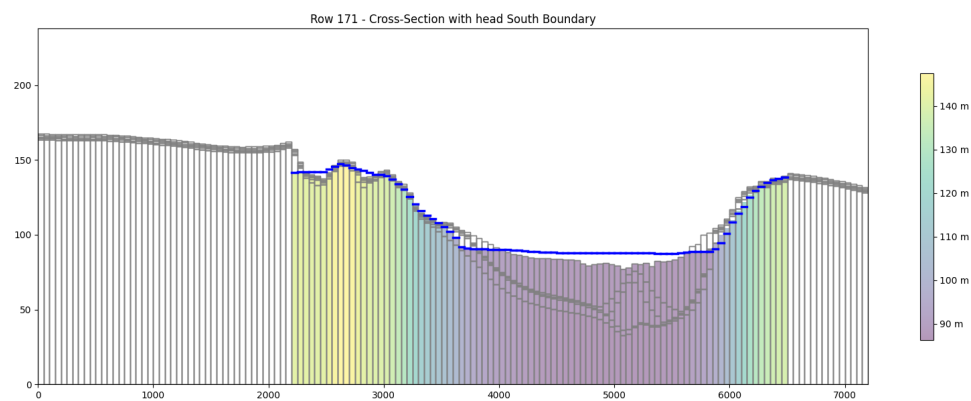
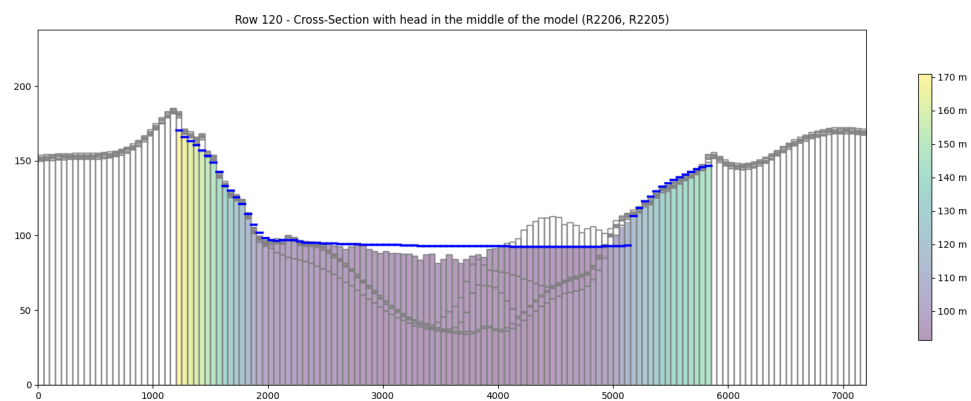
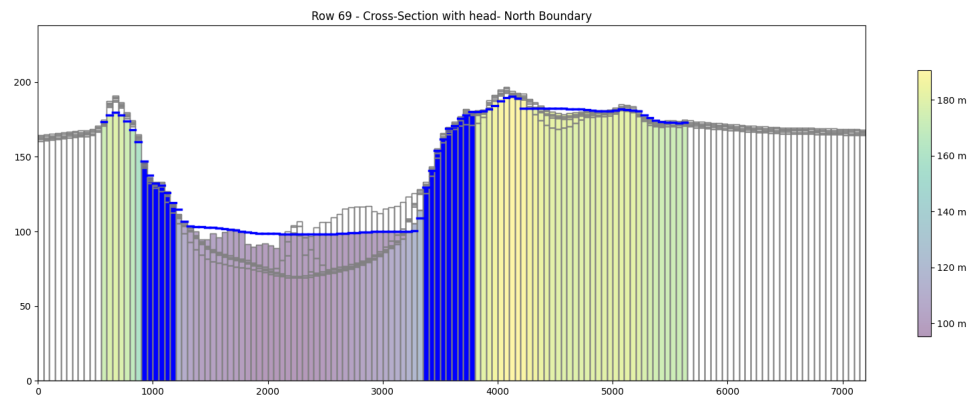


Figure 5.3: Cross-sections (west-east) of model FFS-ND at three different locations in the model.

5.1 Pumping

All models underwent testing by incorporating three pumping wells located in different areas of the model. Pumping caused the head to decrease, i.e. a drawdown. The drawdown is presented as the difference in head before and after pumping. Figure 5.4 depicts the drawdown observed in each well, including the pumping wells, namely B1N, BM4, and B2S. These are exhibiting the most considerable drawdown near their locations. The drawdown is significantly higher in the models without a drain, which are marked with dashed lines in the figure.

The models with the highest drawdown are Models FFS-ND and FFG-ND, which reach a maximum drawdown of 2.1 m. These models have a flow boundary in north (A) and south (B) and a specified or general head in (C), respectively. Additionally, Model SFS-ND had a high drawdown in the south (to the right in the figure) where it has a flow boundary (B). Models FSS-ND, SSS-ND, and GGG-ND have higher drawdown in the middle section, where the difference to the models with a drain is the largest.

The models with the lowest drawdown are the ones with drain. An in-zoomed plot of their drawdown is presented in Figure 5.5. The figure clearly shows the drawdown around the pumping wells. The drawdown is largest around the pumping well (B1N) in the north. In general, Models FFS-D and FFG-D show the highest drawdown compared to the other models with a drain. Model SFS-D shows high values in the south (to the right). Models FSS-D, SSS-D, and GGG-D, shows very similar drawdown throughout the whole model.

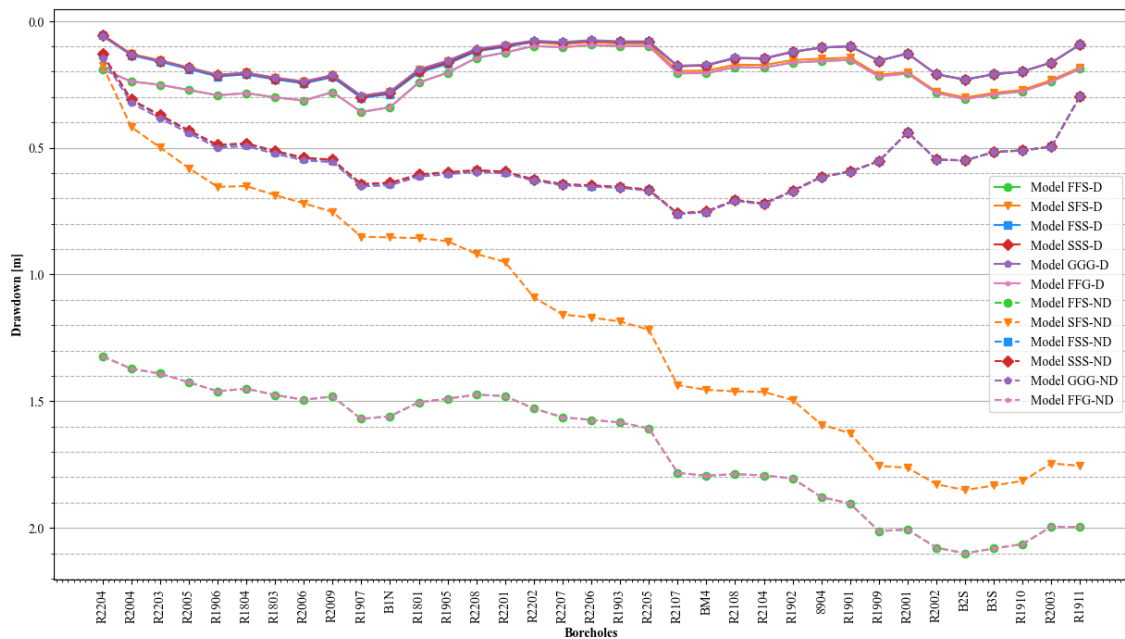


Figure 5.4: Drawdown for all models after pumping in three pumping wells; B1N, BM4 and B2S. Models with drain is marked with solid lines and models without with dashed lines. Models with the same boundary conditions are color matched.

5. Results



Figure 5.5: Drawdown for models with drain included after pumping in three pumping wells; B1N, BM4, B2S.

A contour plot of drawdown in Model FSS-D, which is one of the model with lowest drawdown, is presented in Figure 5.6. The cone of depression is clearly present and shows where the pumping wells are located. The cone of depression is largest for the north and south pumping wells. In Figure 5.7, a similar plot is shown for Model FFS-ND, which has the largest drawdown. In this figure, cone of depression is not as significant as in Figure 5.6, and for the pumping well in the middle, no clear cone of depression is visible.

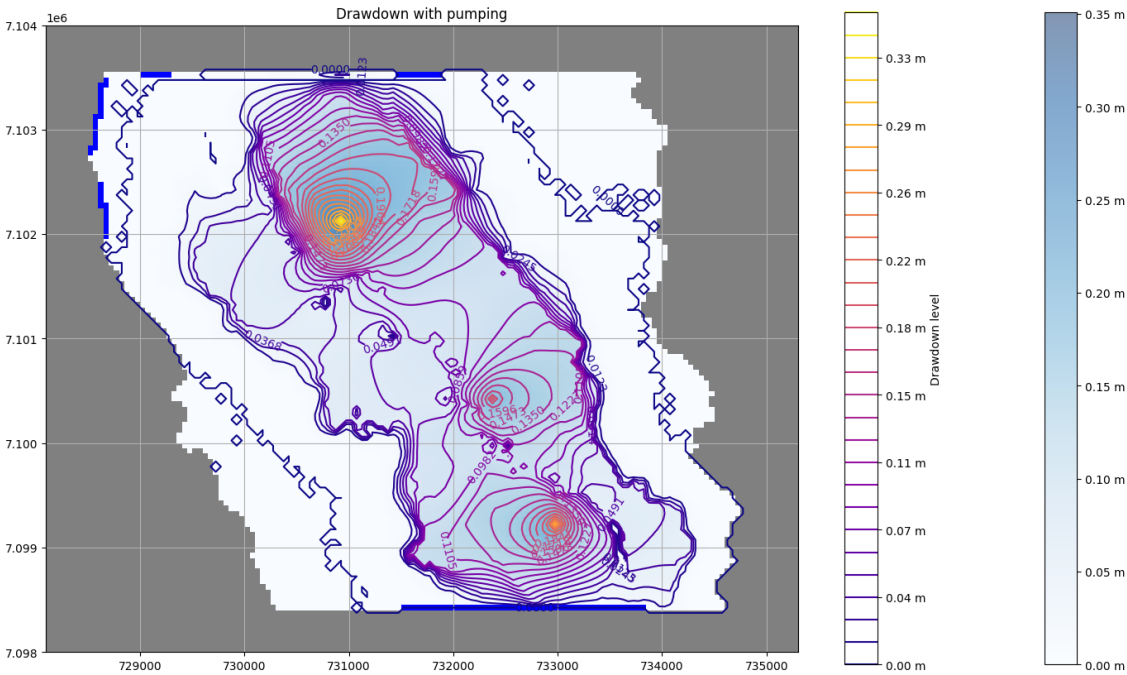


Figure 5.6: Contour plot of drawdown for Model FSS-D. Contours mark the drawdown as lines and a blue color indicates the areas with largest drawdown.

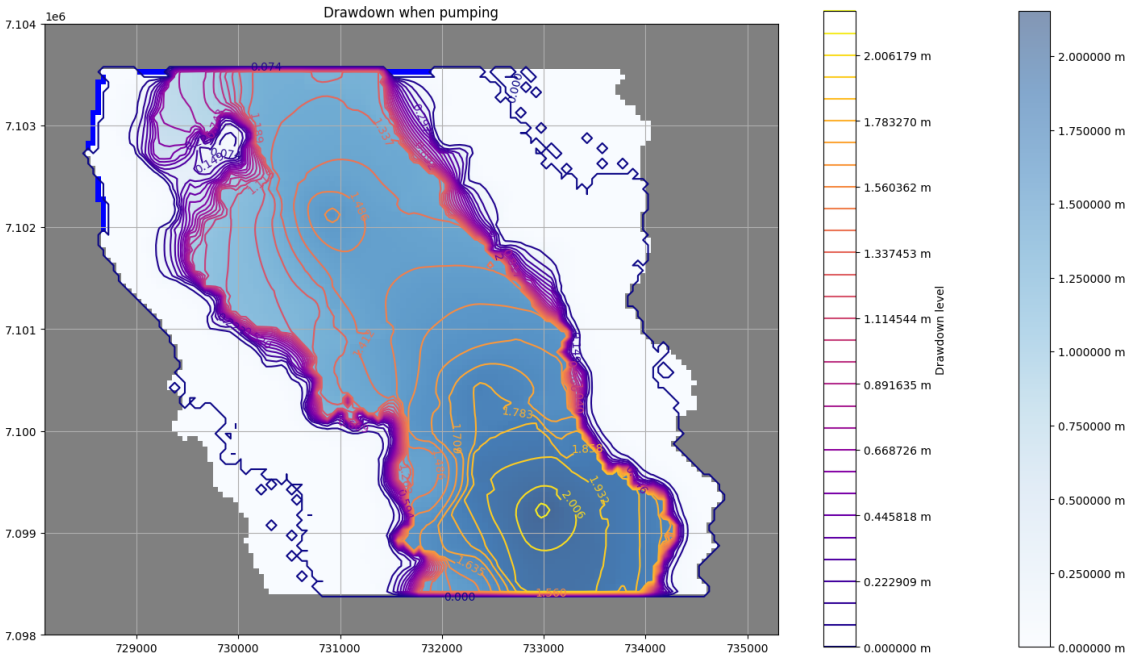


Figure 5.7: Contour plot for drawdown for Model FFS-D. Contours mark the drawdown as lines and a blue color indicates the areas with largest drawdown.

6

Discussion

This chapter contains a sensitivity analysis and a discussion about the model results, including arguments for calibration, how drain and pumping affected the models. Furthermore, the general groundwater modelling process and its largest uncertainties are discussed.

6.1 Calibration

The calibration of the models could have been made in different ways, manually or automatically by using PEST. PEST would have been less time-consuming, however, since the study contains a sensitivity analysis to evaluate the effect of different boundary conditions, the manual calibration was necessary to maintain control over the parameter values. PEST would have compensated the differences between the models, by changing parameter values, in order for the model to simulate groundwater levels that would correspond better to the observed heads. Thus, this compensation would have made the evaluation of the impact from different boundary conditions very difficult or even impossible.

When calibrating the model, values within the intervals, for all parameters, were tested in different combinations. The calibration results showed that the starting heads and recharge made quite a large difference in the model, whereas hydraulic conductivity did not affect the model results significantly, which was surprising.

Assuming the starting heads to be 1 m below the ground surface resulted in very high head output. In order to improve the results, a mix of 1 m below the topography on the outer parts of the area and interpolated heads from the observed head data was tried, which resulted in more realistic head values. As a result, the latter option was used in the final model runs.

When investigating how different hydraulic conductivity values affected the model results, it became apparent that only adjusting K-values did not have a significant impact. When different K-values were assigned in different parts of the model (north, middle and south), each section received unreasonable head values. Moreover, the groundwater levels remained at the same level and did not continuously decrease in accordance with the observed levels, which follow the topography. This resulted in an unnatural drop of the head level between the different parts of the model. Since it is natural for the K-value to vary throughout the area, it was valuable to try to include the variation in the model. However, to divide the area into three parts was not a successful method to include natural variations. Therefore, each soil type had the same K-value throughout the model. Furthermore, it was also concluded that the same K-values could be used for each soil types in all models to be able to focus on investigating the impact of different boundary

conditions.

Using the same recharge value for the entire model resulted in heads consistently reaching above the ground surface, indicating that the inflow and/or precipitation in the model area was too large. To address this issue, recharge was excluded from areas with less permeable materials in the top layer, such as bedrock and fines, as they were considered to have negligible recharge. Conversely, areas with sand and gravel were assumed to receive 350 mm recharge per year, which is 100 % of the annual net precipitation. This approach also proved advantageous in mitigating recharge in regions characterized by steeper slopes, resulting in increased runoff and decreased recharge.

6.2 Conceptual errors

When conceptualising the study area, simplifications, assumptions, and input data was made. This comes with several uncertainties that need to be considered.

When studying the undisturbed model (without pumping) results, it is visible that the simulated heads are higher than the observed head levels along the entire model in all models with the exception of models FFS-D, SFS-D, and FFG-D, which exhibit simulated heads only slightly lower than the observed heads in the south part of the model area. The largest differences between the simulated heads and the observed levels are found in the north part of the model area when studying the model results in the model outcomes incorporating drains. When specified/general heads are used as a boundary condition in the north boundary of the model domain, the levels rise after the first observation well, as can be seen in Figure 5.1. Numerous tests were conducted with different parameter values to lower the simulated heads in the model, however, none of these attempts proved successful. Thus, it is assumed that errors in the conceptualisation have led to the increased head levels.

A significant part of the conceptual model process was the creation of the geological model. As mentioned in Section 3.3 Geological Model Development, several parts of the model may not constitute to a good representation of reality since the interpolation was made automatically. The cross section from Leapfrog, that was presented in Figure 3.9, showed a thick deposit of semi-fines lying on top of the glaciofluvial material that was relatively flat, compared to other parts of the esker. Since the layer of semi-fines is rather permeable, the aquifer almost becomes confined in these parts. The reduced permeability in combination with the thin glaciofluvial material is creating a bottleneck effect in the model, which results in increased water levels and/or localised flooding upstream in the model area. Thus, the presence of a bottleneck effect provides a plausible explanation for the elevated simulated groundwater levels. This is further validated by other studies that has studied the importance of the geological model. Refsgaard et al. (2014) concluded that the dominated source of uncertainty was, in fact, the geology.

Another conceptual error might be that the bedrock layer could have been divided into two distinct layers, with the possibility of assigning a higher K-value to the upper layer. This is a common way to model bedrock since the bedrock usually has more cracks in the upper parts where groundwater could be infiltrated. This could have reduced the head levels in a more natural way. However, the lack of a top bedrock layer was compensated by using a higher K-value for the entire bedrock.

6.3 Sensitivity Analysis of the Impact of Boundary Conditions

When studying the results, it is apparent that all the different boundary condition combinations are possible to use when modelling Umeälsvåsen. However, the results were significantly affected by different boundary conditions. The most significant difference between the models is how Boundary conditions D was defined, whether Tvärån was incorporated as drainage or not. Furthermore, Boundary conditions A and B also contribute to large differences, which are the boundaries that correspond to the regional flow in the esker and are located at the north and south edges of the model area.

The models that include drain, has the largest difference between the models is in north, whereas they follow the same levels in the middle and south part. The largest impact of the drain is in the middle of the models, which could be explained by the distance to the other boundary conditions which affect the models in the edges compared to the drain, that is going through the entire model. When the models were ran without Tvärån, the simulated head seem to follow the observed head curve quite well, however, they were much higher than the observed values. In the cross sections, in Figure 5.3, it could be seen that the heads were several meters above the ground level since the water volume coming into the model was larger than the water coming out of it. However, the problem did not disappear when adjusting the recharge in different surface materials.

Models with flow boundary in the north, and especially in the south (Model FFS-D, Model SSF-D, Model FFG-D), are more dependent on the drain, since they reach the highest head values when drain is not included. Since the flow boundary has specified inflow and outflow, the outflow remains unchanged regardless of any changes in the drain. On the other hand, when using the specified head and general head boundary conditions, the head is set to a specific value. Even if the drain is not included, the head at the boundary remains unchanged. However, in this scenario, more water can flow out of the model in order to maintain the head at the same level. Model GGG-D stands out with a very high head in north, compared to the other models with drain, including the models with specified head in the north, which probably has to do with the head varying with time. The boundary seems to have a higher flow into the model compared to the other boundary conditions in the north.

Since there were no clear signs of a strong connection between Tvärån and the aquifer, it was believed by the experts that the finer materials beneath Tvärån, would result in a weak link. However, each of the six models with drain had a simulated head that was closer to the observed head values, than the six models without drain, which gives the impression that the connection between Tvärån and the esker must be significant. Nevertheless, this would have to be investigated more thoroughly to draw a conclusion. Furthermore, the models were only calibrated with the drain included, which could explain why these models shows a simulated head that is closer to the observed levels. The differences between the models with and without drain is however significant and it is clear that draining by Tvärån is likely. As mentioned in Section 3.1 General Description of Case Study Area, there are some smaller water courses and ponds in the area that are not investigated, which could potentially be of significance as well.

Boundary condition C, where till is located at the surface, are varied between specific head and general head. This boundary condition is compared using Models FFS-D and FFG-D. Since the two models has the same result, it can be concluded that both boundary

conditions could be used in this area.

6.3.1 The Impact of Pumping Event

As a further evaluation in the sensitivity analysis, it is interesting to study the pumping results from the models. Pumping influences the models with different drawdown patterns. The largest drawdown occurs mainly in the southern part of the models. One reason for this is that the southern well has the highest pumping rate. Due to the natural gradient, the hydraulic head is higher in the north and decreases towards the south due to the topography. When pumping simultaneously in all three wells, the drawdown naturally increases along the esker as less water from the north flows towards the south. Additionally, pumping exerts a stronger impact on models without drainage compared to those with drains. It was expected that models with drains, having less initial water, would experience greater drawdown. The unexpected results suggest that there might be additional factors or complexities that influence the behavior of the models. It could also mean that water from Tvärån is contributed as injection to the pumping, which would explain these results. Further investigation would be needed to understand the underlying reasons for this observation. Moreover, this result reinforces the reliance on models with drains.

When studying Figure 5.5, which does not include the models without drain, the largest drawdown could be seen in the north part of the model area. This was not expected, since the drawdown should increase from north to south in these models as well. These unexpected results might be due to the bottleneck effect in the geological model, or other modelling errors.

The models with the lowest drawdown are models FSS-D, SSS-D and GGG-D, which all have specific or general head in south (B) and in north (A), despite model FSS-D which has flow boundary in A. The corresponding models without a drain are models FSS-ND, SSS-ND and GGG-ND, which also have the lowest drawdown compared to all models without a drain. Notably, these models have a higher drawdown in the middle but a lower drawdown in the south, which is because of the boundary condition in the south. Additionally, model FFS-D and FFG-D has the largest drawdown among the models with a drain, and the corresponding model without a drain is model FFS-ND and FFG-ND, which also has the largest drawdown. Model FFS-D and FFG-D have flow boundary in both north and south. Hence, there is a clear distinction between a flow boundary and a head-dependent boundary when pumping.

Additionally, when using specified head or general head, the head needs to be adjusted to account for the water being pumped out of the model. This adjustment is necessary because, otherwise, the flow in the model would be higher in order to compensate for the extracted water. This compensation is one reason for the lower drawdown observed in the model with specific or general head in the south (B). However, the general head boundary is expected to be more accurate than the specific head boundary, as the head can change over time. Moreover, the models with flow boundary may yield more realistic results. However, it is not realistic to assume that the regional flow in the model remains constant when pumping a significant amount of water in or out of the system.

6.3.2 Summary of the Impact of Boundary Conditions

To summarise, a specific head boundary is beneficial to use when groundwater levels are known at the boundary or when groundwater flow is unknown or difficult to measure. However, the specific head remains stable even when the system is stressed, such as during a pumping event, which is not realistic in a natural system. Furthermore, a general head boundary is similar to the specific head boundary but is more adaptable to changes in the system over time. The flow boundary models were difficult to calibrate and control to the same extent as the models with head-dependent boundaries. During a stress event, the head is not controlled by the flow boundary. However, a specific flow is not realistic either, since the groundwater flow also changes when the system is stressed.

6.4 Uncertainties in Groundwater Modelling

The process of groundwater modelling is extensive and it is essential to analyse what kind of uncertainties that are present at the site and in the model, and how much they affect the model results. A sensitivity analysis or an uncertainty analysis can help to understand the errors and uncertainties, and therefore make it possible to develop a more realistic model. This makes it more clear what part of the process that makes the most difference in the model results and it brings knowledge in what parts that need further investigations.

As mentioned in Section 2.2 Conceptual Model, the largest uncertainty in groundwater models comes from the conceptualisation. Based on the analysis of the model results, it became clear that it is essential to get a proper understanding of the system in order to specify the significant parts of the model. Data should, therefore, be assembled and thoroughly analysed. To be able to set the model domain, it is necessary to know how the groundwater flows in the model, so that proper boundary conditions can be used. Furthermore, it was shown that surface water and the connection between surface water and the aquifer can make a large impact on the system. Additionally, if the geological conditions are not known at the site, the model will probably not result in any realistic results. Both the thickness of the soil types and hydrogeological parameters in the materials can make a significant impact on the model. However, since it is rarely possible to know everything about the geological, hydrogeological and hydrological conditions at the site, assumptions need to be made. The assumptions and simplifications will always entail uncertainty to the model, even when they are made by experts with solid reasoning.

After developing a numerical groundwater model, it became clear that it includes many decisions and potentially further simplification of the conceptual model. Since there are numerous methods to write a script that will produce the same outputs, the most suitable option should be used for the specific site that is being modelled. However, this was not always clear and the understanding of the site, as well as personal knowledge in modelling, can limit the numerical model. In Flopy, there are many packages that can be used that are slightly different from each other. It can, therefore, be difficult to understand how the different packages will affect the model results, which leads to numerical model uncertainties. These uncertainties also makes it difficult to control the model output.

6.5 Further Studies

The focus on this study has been to analyse the uncertainties that comes with the choice of boundary conditions that are used in a numerical model. However, this has led to new

questions arising in both the conceptualisation of the site, as well as the choices that were made in the numerical modelling process.

Further studies could be made on Umeälvssäsen in order to obtain a model which is even more in line with reality. Since one of the largest uncertainties in the models is believed to be the geological model, it would be beneficial to make a sensitivity analysis on different geological models. Moreover, boreholes on the sides of the esker would add knowledge on how the geology varies in the study area. It could also be a good idea to introduce one or several more soil types, in order to see how the preciseness of hydrogeological parameters connected to the material could affect the model. Nevertheless, increasing the complexity of models by adding more parameters is not always the optimal solution for improving the model's results. This is because complex models are more difficult to evaluate and identify uncertainties and errors, as they require analyzing and evaluating a larger number of parameters. Additionally, another large uncertainty is where and how drain should be incorporated in the model. This could be clarified by conducting measurements and tests on Tvärån and compare the surface water levels to the groundwater levels in the esker. It could then be interesting to investigate how the model results would be affected if drain from Tvärån was only included where Tvärån crosses the glaciofluvial deposit. Even though the drainage package should take the permeability of the underlying layer into consideration, it is not clear how much water is drained from the more impermeable materials.

In order to decide whether or not the esker should be used as drinking water supply, the model should include the infiltration basins which are planned to be constructed in the area in order to elevate the groundwater levels when pumping large volumes of groundwater from the esker. This would provide valuable insights on the potential impact on the hydrogeology in the area. It is also possible to make a numerical model that would provide insight on the water quality in different parts of the area, which could be useful when evaluating the potential usage of the aquifer of groundwater extraction.

When it comes to the numerical modelling, there are several packages and choices that were made along the process that could have been different. In order to create a simple model that would not take too much computational power and that is more complex than necessary, the grid size was decided to be 50x50 m with a structural (squared) grid. A finer grid size and an unstructured grid would result in a more detailed model that might be closer to reality. However, since a more detailed model could generate more uncertainties and less control of the input, it may not result in a better model. Nevertheless, since this is not investigated in this study, no conclusions can be drawn on this matter without further research. When it comes to packages, it would be interesting to try another solver that would calculate recharge and heads in a different way, which may lead to different results.

7

Conclusion

The aim of this study was to evaluate the effects of different boundary conditions on groundwater modelling using multiple numerical models. To achieve this, several numerical models were developed based on the conceptualisation of the study area. Moreover, this made it possible to assess the impact of model uncertainties. The conceptual model plays a crucial part in the groundwater modelling process, including both an understanding of the groundwater system, as well as simplifications and assumptions. Among the conceptual uncertainties, the geological model stands out as a key factor, as it forms the basis of the model, incorporates various assumptions and uncertainties, and shapes the overall structure of the model.

Furthermore, it can also be concluded that the understanding and information of the water balance in the system is of great importance when analysing the modelling result. Factors such as groundwater levels, recharge, drainage, groundwater flow, and connections to surface water, are all a part of the water balance in the system and they all play essential roles in determining the modelling outcomes. Field investigations and data gathering are essential for developing a comprehensive geological and hydrogeological understanding, and in order to calibrate the model. However, achieving a complete and realistic model of the area is practically impossible due to inherent uncertainties. Thus, it becomes essential to explore different input values in areas with limited conceptual understanding and high levels of uncertainty.

All the boundary condition combinations that were tested are applicable, with the most significant differences emerging during pumping events when the system is stressed. Therefore, careful consideration of the boundary conditions and their properties is crucial, depending on the specific simulation objectives of the model. Additionally, the presence of drainage has a considerable impact on the models and may indicate a significant connection between the groundwater system and Tvärån. However, this would have to be investigated further in order to draw a conclusion.

Uncertainties in the numerical model development appear from parameters and the software packages employed, which are, in turn, based on the conceptual model. Hence, it is advisable to explore different numerical options to identify areas of significant uncertainty and determine the factors that most profoundly affect the results.

While it is impossible to completely eliminate uncertainties arising from assumptions and simplifications in the conceptual model, it is crucial to identify and acknowledge them. Furthermore, experimenting with various combinations of boundary conditions, parameters, and model setups is important in constructing a reasonable groundwater model. Finally, a thorough understanding of the system and the model itself is essential for iden-

tifying uncertainties and recognising their impact on the modelling results.

The final conclusions from the study are:

- The key conceptual uncertainty is the geological model.
- Understanding of the water balance is of great importance.
- All boundary conditions that were tested are applicable but shows different results. Boundary conditions should be decided based on the purpose of the modelling.
- The models with drainage included showed more reasonable results.
- The largest difference between the boundary conditions occurred in the pumping result.

References

- Anderson, M. P., Woessner, W. W., & Hunt, R. J. (2015). *Applied groundwater modeling : simulation of flow and advective transport* (Second Edition ed.).
- ASTM International. (2019). *Standard Guide for Conceptualization and Characterization of Groundwater Systems 1*. Retrieved from www.astm.org. doi: 10.1520/D5979-96R19E01
- Bakker, M., & Post, V. (2022). *Analytical Groundwater Modeling* (1st Edition ed.). CRC Press.
- Bakker, M., Post, V., Langevin, C. D., Hughes, J. D., White, J. T., Starn, J. J., & Fienen, M. N. (2016, 9). Scripting MODFLOW Model Development Using Python and FloPy. *Groundwater*, *54*(5), 733–739. doi: 10.1111/gwat.12413
- Barthel, R., Stangefelt, M., Giese, M., Nygren, M., Seftigen, K., & Chen, D. (2021). Current understanding of groundwater recharge and groundwater drought in Sweden compared to countries with similar geology and climate. *Geografiska Annaler, Series A: Physical Geography*, *103*(4), 323–345. doi: 10.1080/04353676.2021.1969130
- Beisbart, C., & Saam, N. J. (2019). *Simulation Foundations, Methods and Applications Computer Simulation Validation Fundamental Concepts, Methodological Frameworks, and Philosophical Perspectives*. Retrieved from <http://www.springer.com/series/10128>
- Borthakur, A., & Singh, P. (2020). Sustainability science—below and above the ground as per the United Nation’s sustainable development goals. In *Climate change and soil interactions* (pp. 453–471). Elsevier. doi: 10.1016/b978-0-12-818032-7.00017-5
- Boyle, D. P., Gupta, H. V., & Sorooshian, S. (2000). Toward improved calibration of hydrologic models: Combining the strengths of manual and automatic methods. *Water Resources Research*, *36*(12), 3663–3674. doi: 10.1029/2000WR900207
- Brassington, F. C., & Younger, P. L. (2010, 12). A proposed framework for hydrogeological conceptual modelling. *Water and Environment Journal*, *24*(4), 261–273. doi: 10.1111/j.1747-6593.2009.00173.x
- Bredehoeft, J. (2005, 3). The conceptualization model problem - Surprise. *Hydrogeology Journal*, *13*(1), 37–46. doi: 10.1007/s10040-004-0430-5
- Butts, M. B., Payne, J. T., Kristensen, M., & Madsen, H. (2004, 10). An evaluation of the impact of model structure on hydrological modelling uncertainty for streamflow simulation. In *Journal of hydrology* (Vol. 298, pp. 242–266). doi: 10.1016/j.jhydrol.2004.03.042
- Doherty, J. (2003, 3). Ground water model calibration using pilot points and regularization. *Ground Water*, *41*(2), 170–177. doi: 10.1111/j.1745-6584.2003.tb02580.x
- El-Ghonemy, H., Watts, L., & Fowler, L. (2005). Treatment of uncertainty and developing conceptual models for environmental risk assessments and radioactive waste disposal safety cases. *Environment International*, *31*(1), 89–97. doi: 10.1016/j.envint.2004

- .07.002
- Enemark, T., Peeters, L. J., Mallants, D., & Batelaan, O. (2019, 2). Hydrogeological conceptual model building and testing: A review. *Journal of Hydrology*, *569*, 310–329. doi: 10.1016/j.jhydrol.2018.12.007
- Engelhardt, I., De Aguinaga, J. G., Mikat, H., Schüth, C., & Liedl, R. (2014). Complexity vs. Simplicity: Groundwater model ranking using information criteria. *Groundwater*, *52*(4), 573–583. doi: 10.1111/gwat.12080
- Fetter, C. W. C. W. (2014). *Applied hydrogeology*. Pearson.
- Gong, W., Gupta, H. V., Yang, D., Sricharan, K., & Hero, A. O. (2013, 4). Estimating epistemic and aleatory uncertainties during hydrologic modeling: An information theoretic approach. *Water Resources Research*, *49*(4), 2253–2273. doi: 10.1002/wrcr.20161
- Green, R. (1974). *THE SEISMIC REFRACTION METHOD-A REVIEW*.
- Gupta, H. V., Clark, M. P., Vrugt, J. A., Abramowitz, G., & Ye, M. (2012). *Towards a comprehensive assessment of model structural adequacy* (Vol. 48) (No. 8). doi: 10.1029/2011WR011044
- Hamby, D. M. (1994, 9). A review of techniques for parameter sensitivity analysis of environmental models. *Environmental Monitoring and Assessment*, *32*(2), 135–154. doi: 10.1007/BF00547132
- Leaf, A. T., & Fienen, M. N. (2022, 9). Modflow-setup: Robust automation of groundwater model construction. *Frontiers in Earth Science*, *10*. doi: 10.3389/feart.2022.903965
- Paz, C., Alcalá, F. J., Carvalho, J. M., & Ribeiro, L. (2017, 10). *Current uses of ground penetrating radar in groundwater-dependent ecosystems research* (Vol. 595). Elsevier B.V. doi: 10.1016/j.scitotenv.2017.03.210
- Ramboll. (2022, 2). *Reservvattentäkt Umeå - Fas 1* (Tech. Rep.). Retrieved from <https://se.ramboll.com>
- Refsgaard, J. C., Auken, E., Bamberg, C. A., Christensen, B. S., Clausen, T., Dalgaard, E., ... Viezzoli, A. (2014, 1). Nitrate reduction in geologically heterogeneous catchments - A framework for assessing the scale of predictive capability of hydrological models. *Science of the Total Environment*, *468-469*, 1278–1288. doi: 10.1016/j.scitotenv.2013.07.042
- Refsgaard, J. C., van der Sluijs, J. P., Brown, J., & van der Keur, P. (2006, 11). A framework for dealing with uncertainty due to model structure error. *Advances in Water Resources*, *29*(11), 1586–1597. doi: 10.1016/j.advwatres.2005.11.013
- Refsgaard, J. C., van der Sluijs, J. P., Højberg, A. L., & Vanrolleghem, P. A. (2007, 11). Uncertainty in the environmental modelling process - A framework and guidance. *Environmental Modelling and Software*, *22*(11), 1543–1556. doi: 10.1016/j.envsoft.2007.02.004
- Rojas, R., Kahunde, S., Peeters, L., Batelaan, O., Feyen, L., & Dassargues, A. (2010, 11). Application of a multimodel approach to account for conceptual model and scenario uncertainties in groundwater modelling. *Journal of Hydrology*, *394*(3-4), 416–435. doi: 10.1016/j.jhydrol.2010.09.016
- Saltelli, A., Ratto, M., Tarantola, S., & Campolongo, F. (2006, 10). *Sensitivity analysis practices: Strategies for model-based inference* (Vol. 91) (No. 10-11). doi: 10.1016/j.res.2005.11.014
- Samani, S., Moghaddam, A. A., & Ye, M. (2018, 3). Investigating the effect of complexity on groundwater flow modeling uncertainty. *Stochastic Environmental Research and Risk Assessment*, *32*(3), 643–659. doi: 10.1007/s00477-017-1436-6
- Sebok, E., Refsgaard, J. C., Warmink, J. J., Stisen, S., & Jensen, K. H. (2016, 7).

- Using expert elicitation to quantify catchment water balances and their uncertainties. *Water Resources Research*, 52(7), 5111–5131. doi: 10.1002/2015WR018461
- SGU. (n.d.). *Hydraulisk konduktivitet i berg*. Retrieved from <https://apps.sgu.se/kartvisare/kartvisare-hydraulisk-konduktivitet.html>
- SMHI. (n.d.). *Nederbörd*. Retrieved from <https://www.smhi.se/data/meteorologi/nederbord>
- Svenskt Vatten. (2016, 5). *Produktion av dricksvatten*. Retrieved from <https://www.svensktvatten.se/fakta-om-vatten/dricksvattenfakta/produktion-av-dricksvatten/>
- Svenskt Vatten. (2019, 12). *Reningsprocesser i vattenverk*. Retrieved from <https://www.svensktvatten.se/vattentjanster/dricksvatten/vattenverk-och-reningsprocesser/reningsprocesser-i-vattenverk/>
- Tonkin, M., & Doherty, J. (2009, 12). Calibration-constrained Monte Carlo analysis of highly parameterized models using subspace techniques. *Water Resources Research*, 45(12). doi: 10.1029/2007WR006678
- United Nations. (2022). *The Sustainable Development Goals Report*.
- U.S. Geological Survey. (2018, 6). *Where is Earth's Water?* Retrieved from <https://www.usgs.gov/special-topics/water-science-school/science/where-earths-water>
- USGS. (n.d.). Boundary Conditions. Retrieved from https://water.usgs.gov/nrp/gwsoftware/ModelMuse/Help/boundary_conditions5.html
- USGS. (2022). *Online Guide to MODFLOW-2005*.
- Walker, D., Baumgartner, D., Gerba, C., & Fitzsimmons, K. (2019). Surface Water Pollution. In *Environmental and pollution science* (pp. 261–292). Elsevier. doi: 10.1016/b978-0-12-814719-1.00016-1
- Walker, W., Harremoës, P., Rotmans, J., van der Sluijs, J., van Asselt, M., Janssen, P., & Kreyer von Krauss, M. (2003, 3). Defining Uncertainty: A Conceptual Basis for Uncertainty Management in Model-Based Decision Support. *Integrated Assessment*, 4(1), 5–17. doi: 10.1076/iaij.4.1.5.16466
- Wikner, T. (2006). *Beskrivning till karta över grundvattenförekomster i Umeå kommun*. Uppsala.
- Wikner, T., Müllern, C.-F., Rurling, S., & Thunholm, B. (2002a). *Grundvattenkartor Beskrivning till kartan över grundvattnet i Västerbottens län*. Uppsala.
- Wikner, T., Müllern, C.-F., Rurling, S., & Thunholm, B. (2002b). *Uppsala 2002 Grundvattenkartor Beskrivning till kartan över grundvattnet i Västerbottens län*.
- Zheng, C., & Bennett, G. D. (1995, 7). Applied Contaminant Transport Modeling: Theory and Practice. *Journal of Environmental Quality*, 25(4), 927–927. doi: 10.2134/jeq1996.00472425002500040045x
- Zhou, Y., & Herath, H. M. (2017, 5). Evaluation of alternative conceptual models for groundwater modelling. *Geoscience Frontiers*, 8(3), 437–443. doi: 10.1016/j.gsf.2016.02.002

A

Appendix A - Calibration Results

Table A.1: Final hydraulic conductivity for each soil type.

Soil type	Hydraulic Conductivity [m/d]
Fines	0.436
Semi-fines	100
Sand	362
Gravel	671
Till	0.864
Bedrock	0.0475

The final recharge percentages, after testing different values and variations, are presented in Table A.2. Furthermore, the lowest inflow and outflow

Table A.2: Share of recharge for each soil type. 100 % is 350 mm / year.

Soil type	Recharge
Fines	2%
Semi-fines	80%
Sand	100%
Gravel	100%
Till	30%
Bedrock	2%

Table A.3: Assigned inflow and outflow in the models with flow boundary.

	Inflow [m ³ /d]	Outflow [m ³ /d]
Model FFS-D, -ND	6480	-15120
Model SFS-D, -ND		-15120
Model FSS-D, -ND	6480	
Model SSS-D, -ND		
Model GGG-D, -ND		
Model FFG-D, -ND	6480	-15120

Table A.4: Conductance for drainage.

Models	Conductance [m²/d]
All models	3000

Table A.5: Pumping rate in the three pumping wells in North, Middle and South. Presented in both l/s and m^3/d .

	Pumping rate [l/s]	Pumping rate[m³/d]
North	55	4752
Middle	45	3888
South	75	6480

B

Appendix B - Flopy Script

Groundwater model Vännäs

```
In [1]: # Assign name of the simulation
test_name = "Test"
```

Import packages

```
In [2]: # Import necessary packages
import os
import flopy
import numpy as np
import pandas as pd
import matplotlib.pyplot as plt
from scipy.interpolate import griddata
from shapely.geometry import Polygon
import flopy.utils.binaryfile as bf

from scipy.stats import norm
import math
import statistics

import sys
import os
from tempfile import TemporaryDirectory

# Print Numpy and Flopy versions
print("numpy version: {}".format(np.__version__))
print("flopy version: {}".format(flopy.__version__))

numpy version: 1.22.3
flopy version: 3.3.6
```

Load Existing MODFLOW model from Leapfrog

```
In [3]: # Create a new model workspace folder for the simulation
model_ws = "../" + test_name
os.mkdir(model_ws)
```

```
In [4]: #Load the modflow model
mf = flopy.modflow.Modflow.load(
    '../MODFLOW_Simulation_50x50.nam',
    version='mf2005',
    exe_name='../Exe/mf2005.exe',
    verbose = False,
    model_ws=model_ws,
    load_only = ["DIS"]
)#Load only the DIS package (The model includes several package)
```

```
In [5]: # Check package list included in the model
mf.get_package_list()
```

```
Out[5]: ['DIS']
```

```
In [6]: # Set the model coordinate information
# Lower left corner:
```

```
x11 = 728100.000
y11 = 7095000.000
epsg = 3006
grid = mf.modelgrid
grid.set_coord_info(xoff=x11, yoff=y11, epsg=3006)
grid.extent
# Plot model grid
mf.modelgrid

# Check the DIS package
mf.dis.check()

# Print the model to see what is included
print(mf)
```

DIS PACKAGE DATA VALIDATION:

424 Errors:

424 instances of thin cells (less than checker threshold of 1.0)

Checks that passed:

zero or negative thickness
nan values in top array
nan values in bottom array

MODFLOW 5 layer(s) 240 row(s) 144 column(s) 1 stress period(s)

Assign Parameters

Assign hydraulic conductivity

```
In [7]: hk_fines = 0.436
hk_semifines = 100
hk_sand = 362
hk_gravel = 671
hk_till = 0.8640
hk_bedrock = 0.0475

vk_fines = hk_fines / 2
vk_semifines = hk_semifines
vk_sand = hk_sand
vk_gravel = hk_gravel
vk_till = hk_till
vk_bedrock = hk_bedrock
```

Assign Flow and Conductance

```
In [8]: Inflow = 6480 ## m/d = 75 L/s
Outflow = -15120 ## m/d # 175 L/S

#Share of inflow in each soil type
inflow_gravel_share = 0.53
inflow_sand_share = 0.45
inflow_till_share = 0.02

#Share of outflow in each soil type
outflow_gravel_share = 0.53
outflow_sand_share = 0.45
outflow_semifines_share = 0.02
outflow_till_share = 0
```

```
# Conductance (m2/d)
cond = 3000
```

Assign Recharge

```
In [9]: rech = 350 #mm/year
rech_bedrock = (rech/1000/365)*0.02 # 2 %
rech_till = (rech/1000/365)*0.3 # 30 %
rech_fines = (rech/1000/365)*0.02 # 2 %
rech_semifines = (rech/1000/365)*0.8 # 80 %
rech_gravel_sand = (rech/1000/365) # 100 %
```

Save all parameter to text-file

```
In [10]: variables = {
    "Inflow = ": Inflow,
    "Outflow = ": Outflow,
    "cond = ": cond,
    "inflow_gravel_share = ": inflow_gravel_share,
    "inflow_sand_share = ": inflow_sand_share,
    "inflow_till_share = ": inflow_till_share,
    "outflow_gravel_share = ": outflow_gravel_share,
    "outflow_sand_share = ": outflow_sand_share,
    "outflow_semifines_share = " : outflow_semifines_share,
    "outflow_till_share = " : outflow_till_share,
    "rech = ": rech,
    "rech_bedrock = ":rech_bedrock,
    "rech_till = ":rech_till,
    "rech_fines = ":rech_fines,
    "rech_semifines = ":rech_semifines,
    "rech_gravel_sand = ":rech_gravel_sand,
    "hk_fines = ": hk_fines,
    "hk_semifines = " :hk_semifines,
    "hk_sand = " : hk_sand,
    "hk_gravel = " : hk_gravel,
    "hk_till = " : hk_till,
    "hk_bedrock = " : hk_bedrock,
}

with open(model_ws + '/variables_' + test_name + '.csv', 'w') as f:
    for key in variables.keys():
        f.write("%s,%s\n"%(key,variables[key]))
```

Import CSV file from QGIS

```
In [11]: # Open data location:
Data = pd.read_csv('../Model_flow_boundary_NS.csv', low_memory=False)
Data.head()
```

```
Out[11]:
```

	node	row	column	botm_1	botm_2	botm_3	botm_4	botm_5	top	ibou
0	1	1	1	200.967300	199.967300	198.967300	197.967300	0.0	201.967300	
1	2	1	2	200.257797	199.257797	198.257797	197.257797	0.0	201.257797	
2	3	1	3	199.548294	198.548294	197.548294	196.548294	0.0	200.548294	
3	4	1	4	198.838898	197.838898	196.838898	195.838898	0.0	199.838898	
4	5	1	5	198.129395	197.129395	196.129395	195.129395	0.0	199.129395	

5 rows × 58 columns

```
In [12]: # Read out data values from the csv file.
# Csv file is created in QGIS to assign values
#to specific cells and layers.
node = Data['node'].values
top = Data['top'].values
row = Data['row'].values
column = Data['column'].values
botm_1 = Data['botm_1'].values
botm_2 = Data['botm_2'].values
botm_3 = Data['botm_3'].values
botm_4 = Data['botm_4'].values
botm_5 = Data['botm_5'].values
ibound_1 = Data['ibound_1'].values
ibound_2 = Data['ibound_2'].values
ibound_3 = Data['ibound_3'].values
ibound_4 = Data['ibound_4'].values
ibound_5 = Data['ibound_5'].values
shb = Data['shb_till'].values
strt_1 = Data['strt_1'].values
Data.shape
```

Out[12]: (34560, 58)

Groundwater levels - Interpolation

```
In [13]: # Open starting head location. Interpolerad data från QGIS
GV = pd.read_csv('../GV_interpolering.csv', low_memory=False)
GV.head()
```

```
Out[13]:
```

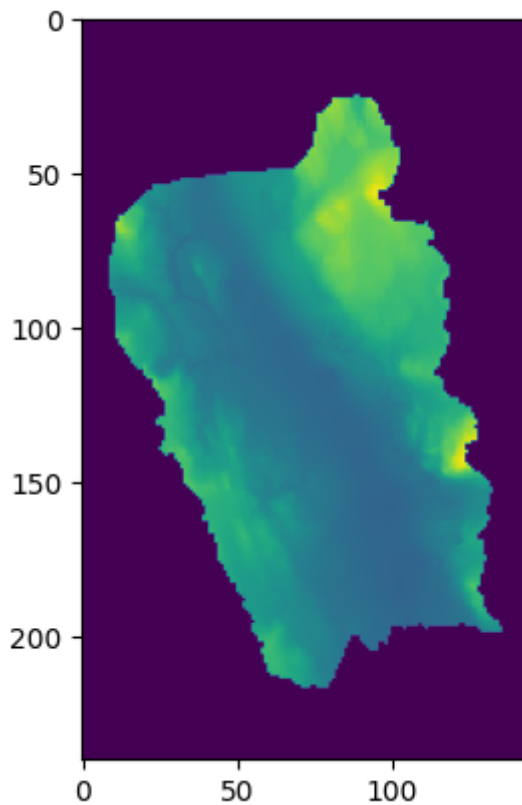
	Y	X	fid	VALUE
0	7105727	728535	1	0.0
1	7105727	728585	2	0.0
2	7105727	728635	3	0.0
3	7105727	728685	4	0.0
4	7105727	728735	5	0.0

```
In [14]: # Assign the interpolation to GV_Value_Grid as starting head
GV_value = GV['VALUE'].values
GV_value_grid = GV_value.reshape((192,128))

GV_interpolation = np.zeros([240, 144])
```

```
GV_interpolation[25:217,8:136] = GV_value_grid
plt.imshow(GV_interpolation)
```

Out[14]: <matplotlib.image.AxesImage at 0x207f0c82e20>



Reshape Data

```
In [15]: # Reshape Data to the same shape as the grid.
grid_top = top.reshape((240,144))
grid_shb = shb.reshape((240,144))
row_grid = row.reshape((240,144))
column_grid = column.reshape((240,144))
iboundData1 = ibound_1.reshape((240,144))
iboundData2 = ibound_2.reshape((240,144))
iboundData3 = ibound_3.reshape((240,144))
iboundData4 = ibound_4.reshape((240,144))
iboundData5 = ibound_5.reshape((240,144))
grid_strt_1 = strt_1.reshape((240,144))
```

Define soiltype to all cells

```
In [16]: # Define the number of Layers, Rows and Columns in the grid
nLays = grid.shape[0]
nCols = grid.shape[2]
nRows = grid.shape[1]
cellH = 50

print("nCols:", nCols)
print("nRows:", nRows)
print("nLays:", nLays)
```

nCols: 144
 nRows: 240
 nLays: 5

```
In [17]: #cell_type - Read out soil type as cell_type from
# the .zon file exported from the Leapfrog model
path = ".../MODFLOW_Simulation_50x50.zon"

layer = -1
layer_data = []

with open(path, 'r') as f:
    for line in f:
        if line[0] == '#':
            continue
        elif line.strip()[:-2] == 'INTERNAL 1 (FREE) -1 lithologies for layer':
            layer += 1
            continue
        if layer >= 0:
            try:
                for i in line.strip().split(' '):
                    layer_data.append(int(i))
            except ValueError:
                continue

cell_type = np.array(layer_data).reshape((5,240,144))
```

Add packages to the model

DIS package

```
In [18]: dis = flopy.modflow.ModflowDis.load(
    model=mf,
    f='MODFLOW_Simulation_50x50.dis')
mf.dis.check()
```

DIS PACKAGE DATA VALIDATION:

424 Errors:

424 instances of thin cells (less than checker threshold of 1.0)

Checks that passed:

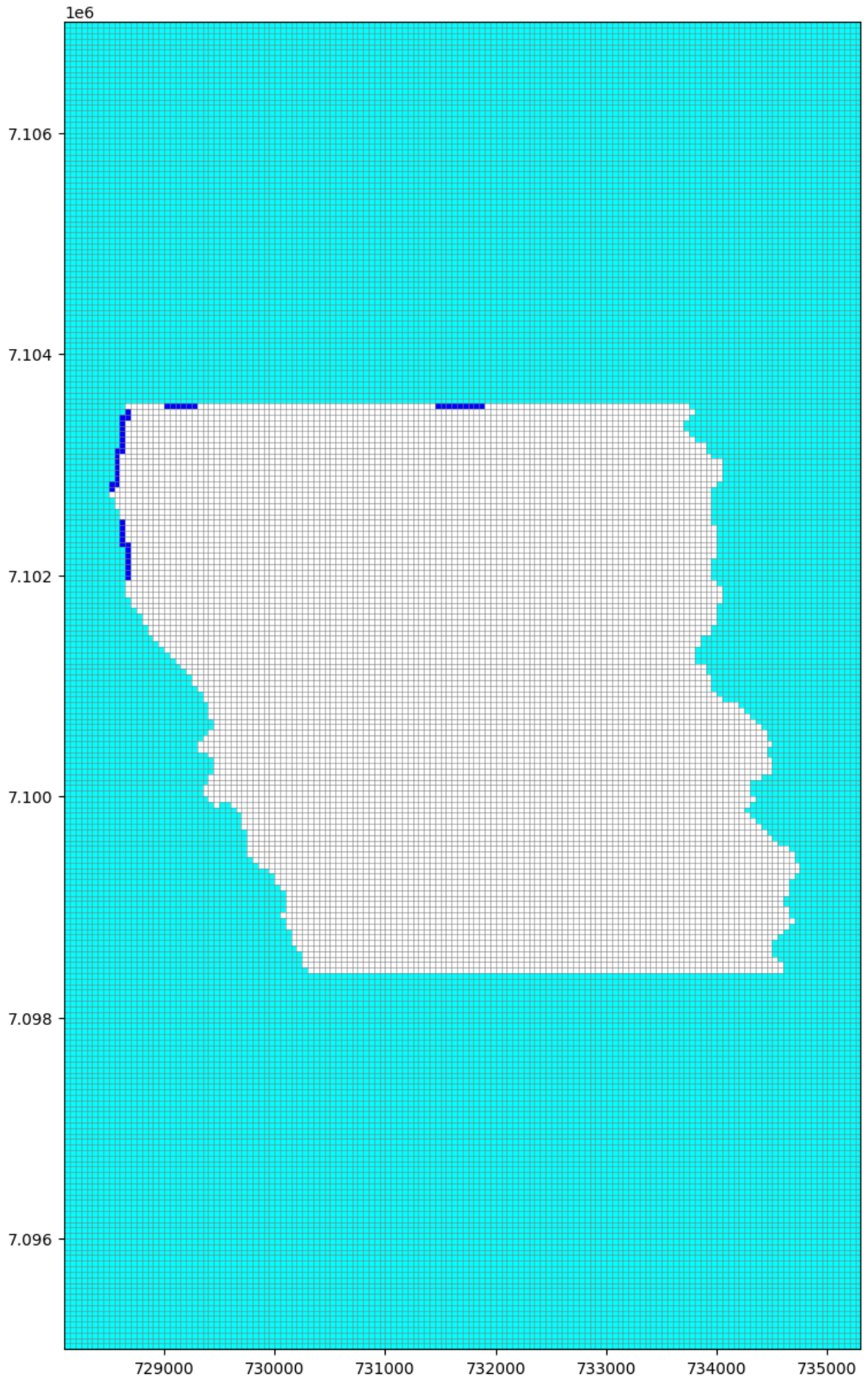
zero or negative thickness
 nan values in top array
 nan values in bottom array

```
Out[18]: <flopy.utils.check.check at 0x207f0e7a7c0>
```

BAS Package

```
In [19]: ibound = [iboundData1,iboundData2,iboundData3,iboundData4,iboundData5]
strt = GV_interpolation
bas = flopy.modflow.ModflowBas(model=mf,ibound=ibound,strt=strt, ichflg = True)

# Plot Ibound (Active and Inactive cells)
fig = plt.figure(figsize=(15, 15))
ax = fig.add_subplot(1, 1, 1, aspect='equal')
modelmap = flopy.plot.PlotMapView(model=mf)
quadmesh = modelmap.plot_ibound(color_noflow='cyan')
linecollection = modelmap.plot_grid(linewidth=0.4)
```



Flow Head Boundary

```

In [20]: # Find cells with glaciofluvial deposits (Gravel and Sand)
# Gravel = Cell_type == 5
# Sand = Cell_type == 4
# Till = Cell_type == 6

#Create a empty array to fill with the cells Located in the For Loop

#Inflow (North)
flow_boundary = []
for layer in range(cell_type.shape[0]):
    row = 69
    for col in range(27,66):

        if cell_type[layer,row,col] == 5:
            flow_boundary.append([layer,row,col,0,
                                (Inflow*inflow_gravel_share)/5])
        elif cell_type[layer,row,col] == 4:
            flow_boundary.append([layer,row,col,0,
                                (Inflow*inflow_sand_share)/36])
        elif cell_type[layer,row,col] == 6:
            flow_boundary.append([layer,row,col,0,
                                (Inflow*inflow_till_share)/24])

#Outflow (South)
for layer in range(cell_type.shape[0]):
    row = 171
    for col in range(68,115):

        if cell_type[layer,row,col] == 5:
            flow_boundary.append([layer,row,col,0,
                                (Outflow*outflow_gravel_share)/13])
        elif cell_type[layer,row,col] == 4:
            flow_boundary.append([layer,row,col,0,
                                (Outflow*outflow_sand_share)/20])
        elif cell_type[layer,row,col] == 6:
            flow_boundary.append([layer,row,col,0,
                                (Outflow*outflow_till_share)/61])
        elif cell_type[layer,row,col] == 3:
            flow_boundary.append([layer,row,col,0,
                                (Outflow*outflow_semifines_share)/72])

```

```

In [21]: # Open staring head location in the TILL.

Head_till = pd.read_csv('../shb_till_R2204.csv', low_memory=False)
Head_till.head()

row_30 = Head_till['row'].values
column_30 = Head_till['column'].values
shb_till = Head_till['shb_till'].values

# Define Dataset 7 as the input with specific head in the package.
ds7 = np.zeros([45,5])
ds7[:,1] = row_30
ds7[:,2] = column_30
ds7[:,4] = shb_till

# Define Dataset 7 as the input with specific head in the package.
ds7 = np.zeros([45,5])
ds7[:,1] = row_30
ds7[:,2] = column_30
ds7[:,4] = shb_till

# number of cells with specific head and flow

```

```
nhead = 45
nflow = 231
```

```
In [22]: fhb = flopy.modflow.ModflowFhb(mf,
                                         nbdtim=1,
                                         nflw = nflow,
                                         nhed=nhead,
                                         ifhbss=1,
                                         ds5=flow_boundary,
                                         ds7=ds7)
```

Layer-Property Flow Package

```
In [23]: # Assign hydraulic conductivity to all cell_types
hk = np.zeros([nLays, nRows, nCols])
for layer in range(cell_type.shape[0]):
    for row in range (cell_type.shape[1]):           ## Zone North
        for col in range(cell_type.shape[2]):

            if cell_type[layer,row,col] == 2:       # Fines
                hk[layer,row,col] = hk_fines
            elif cell_type[layer,row,col] == 3:     # Semi-Fines
                hk[layer,row,col] = hk_semifines
            elif cell_type[layer,row,col] == 4:     # Sand
                hk[layer,row,col] = hk_sand
            elif cell_type[layer,row,col] == 5:     # Gravel
                hk[layer,row,col] = hk_gravel
            elif cell_type[layer,row,col] == 6:     # Till
                hk[layer,row,col] = hk_till
            elif cell_type[layer,row,col] == 7:     # Till
                hk[layer,row,col] = hk_bedrock

# Assign vertical hydraulic conductivity to all cell_types
vk = np.zeros([nLays, nRows, nCols])
for layer in range(cell_type.shape[0]):
    for row in range (cell_type.shape[1]):           ## Zone North
        for col in range(cell_type.shape[2]):

            if cell_type[layer,row,col] == 2:       # Fines
                vk[layer,row,col] = vk_fines
            elif cell_type[layer,row,col] == 3:     # Semi-Fines
                vk[layer,row,col] = vk_semifines
            elif cell_type[layer,row,col] == 4:     # Sand
                vk[layer,row,col] = vk_sand
            elif cell_type[layer,row,col] == 5:     # Gravel
                vk[layer,row,col] = vk_gravel
            elif cell_type[layer,row,col] == 6:     # Till
                vk[layer,row,col] = vk_till
            elif cell_type[layer,row,col] == 7:     # Till
                vk[layer,row,col] = vk_bedrock
```

```
In [24]: # Add LPF package to add hydraulic conductivity: Layer-Property Flow Package
lpf = flopy.modflow.ModflowLpf(mf, hk=hk, vka=vk, ipakcb=53)
```

Recharge

```
In [25]: #Create a empty array to fill with the cells located in the For Loop

recharge_zone = np.zeros((240,144))
for row in range (69,171):
```

```

for col in range(cell_type.shape[2]):

    if cell_type[0,row,col] == 7:           # Bedrock
        recharge_zone[row,col] = rech_bedrock
    elif cell_type[0,row,col] == 2:       # Fines
        recharge_zone[row,col] = rech_fines
    elif cell_type[0,row,col] == 3:       # Semi-Fines
        recharge_zone[row,col] = rech_semifines
    elif cell_type[0,row,col] == 4:       # Sand
        recharge_zone[row,col] = rech_gravel_sand
    elif cell_type[0,row,col] == 5:       # Gravel
        recharge_zone[row,col] = rech_gravel_sand
    elif cell_type[0,row,col] == 6:       # Till
        recharge_zone[row,col] = rech_till

```

```
In [26]: rch = flopy.modflow.ModflowRch(mf, rech=recharge_zone, nrchop = 1, ipakcb=53)
```

Pumping Well

```

In [27]: #Add pumping well
         #We will pump continuously

         #Norr = 55 L/s = 4752 m3/d
         #Mitt = 45 L/s = 3888 m3/d
         #Söder = 75 L/s = 6480 m3/d

         Q_pump_north = -4752 #m3/day (extract water (-))
         Q_pump_middle = -3888
         Q_pump_south = -6480
         stress_period_well = {0:[[2, 97, 56, Q_pump_north],
                                   [2, 131, 85, Q_pump_middle],
                                   [2, 155, 97, Q_pump_south]]}
         #stress/Time period [Lay,row,column,flux]

         wel = flopy.modflow.ModflowWel(mf, stress_period_data = stress_period_well)

```

Drain

```

In [28]: # Open drain cell
         Drain = pd.read_csv('../drain_tvaran_50m.csv', low_memory=False)
         Drain.head()

```

```

Out[28]:
   node  row  column  top  z  c
0  9978   70    42  88.665909  87.665909  3456
1  10113  71    33  99.033234  98.033234  3456
2  10114  71    34  91.744812  90.744812  3456
3  10116  71    36  87.643806  86.643806  3456
4  10117  71    37  87.825630  86.825630  3456

```

```

In [29]: drain_layer = np.zeros(243)
         drain_row = Drain['row'].values
         drain_col = Drain['column'].values
         drain_z = Drain['z'].values
         drain_c = Drain['c'].values

         for i in range(len(drain_c)):

```

```

drain_c[i] = cond # change conductance [m2/d]

spd_DRN = {0: np.column_stack([drain_layer,
                              drain_row,
                              drain_col,
                              drain_z,
                              drain_c]), }

drn = flopy.modflow.ModflowDrn(mf, stress_period_data=spd_DRN)

```

Output control package

```

In [30]: # Add OC package - Output control
#the stress period dictionary is used to set what output is saved
#for the corresponding stress period and time step.
#In this case, the tuple (0, 0) means that stress period 1 and
#time step 1 for MODFLOW will have output saved.
#Head and budgets will be printed and head and budget information will be saved.
spd = {(0, 0): ['print head', 'print budget', 'save head', 'save budget']}
oc = flopy.modflow.ModflowOc(mf, stress_period_data=spd, compact=True)

```

Run the model

```

In [31]: # Add PCG package
#"PCG" which is the most common solver to apply in MODFLOW
pcg = flopy.modflow.ModflowPcg(mf)

```

Write input and run model

```

In [32]: mf.write_input()

```

```

In [33]: mf.run_model()

```

FloPy is using the following executable to run the model: P:/GP_Water/_Admin_Vattnresurs/Teknik/Exjobb_KlaraJosefin/Modelling/Input_Files/Exe/mf2005.exe

```

MODFLOW-2005
U.S. GEOLOGICAL SURVEY MODULAR FINITE-DIFFERENCE GROUND-WATER FLOW MODEL
Version 1.12.00 2/3/2017

```

```

Using NAME file: MODFLOW_Simulation_50x50.nam
Run start date and time (yyyy/mm/dd hh:mm:ss): 2023/05/23 8:21:52

```

```

Solving: Stress period: 1 Time step: 1 Ground-Water Flow Eqn.
Run end date and time (yyyy/mm/dd hh:mm:ss): 2023/05/23 8:22:01
Elapsed run time: 8.716 Seconds

```

```

Normal termination of simulation
(True, [])

```

```

Out[33]:

```

Post-Processing the results

```

In [34]: # Load the head file
head_file_path = os.path.join(model_ws, "MODFLOW_simulation_50x50.hds")
hds = flopy.utils.binaryfile.HeadFile(head_file_path)

```

```
times = hds.get_times()
head = hds.get_data(totim=1.0)
```

```
In [35]: #Read out the CellBudget file (the flow file for each cell at each timestep)
budget_file_path = os.path.join(model_ws, 'MODFLOW_simulation_50x50.cbc')
cbb = flopy.utils.CellBudgetFile(budget_file_path)
kstpker_list = cbb.get_kstpker()
frf = cbb.get_data(text = 'FLOW RIGHT FACE', totim=times[-1])[0]
fff = cbb.get_data(text = 'FLOW FRONT FACE', totim=times[-1])[0]
```

DEPARTMENT OF SOME SUBJECT OR TECHNOLOGY
CHALMERS UNIVERSITY OF TECHNOLOGY
Gothenburg, Sweden
www.chalmers.se



CHALMERS
UNIVERSITY OF TECHNOLOGY